AD-751 785

A STUDY OF ION TRAJECTORIES IN POTENTIAL FLOWS

Michael R. Deluca, et al

Ohio State University
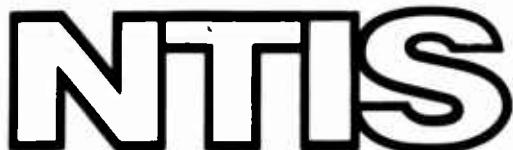
DOCUMENT CONTROL DATA · R & D

(Security classification of title, body of abstract and indexing annotation must be entered when the overall report is classified)

1. ORIGINATING ACTIVITY *(Corporate author)*	2a. REPORT SECURITY CLASSIFICATION
The Ohio State University Research Foundation 1314 Kinnear Rd. Columbus, Ohio 43212	Unclassified
	2b. GROUP
	N/A

3. REPORT TITLE

A STUDY OF ION TRAJECTORIES IN POTENTIAL FLOWS

4. DESCRIPTIVE NOTES *(Type of report and inclusive dates)*

Interim   Technical

5. AUTHOR(S) *(First name, middle initial, last name)*

Michael R. Deluca   H. R. Velkoff

6. REPORT DATE	7a. TOTAL NO. OF PAGES	7b. NO. OF REFS
July 1972	114	17
8a. CONTRACT OR GRANT NO. DA-31-124-ARO-D-246 b. PROJECT NO. 20010501B700 c. 1D12140A142 d.	9a. ORIGINATOR'S REPORT NUMBER(S) Technical Report #11 9b. OTHER REPORT NO(S) *(Any other numbers that may be assigned this report)*

10. DISTRIBUTION STATEMENT

Approved for public release; distribution unlimited.

11. SUPPLEMENTARY NOTES	12. SPONSORING MILITARY ACTIVITY U.S. Army Research Office - Durham Box CM, Duke Station Durham, North Carolina 27706

13. ABSTRACT

An analytical investigation of the motion of ions in a fluid was conducted to provide insight in the use of ions as a fluid flow diagnostic tool. Assuming small space charge density, potential fields and flows were considered. The specific cases studied were fine corona wire to a circular cylinder. Both steady and non-steady flows were considered, and the trajectories of the ions leaving the corona wire were mapped.

IA

DD FORM 1473
1 NOV 65

14 KEY WORDS	LINK A		LINK B		LINK C	
	ROLE	WT	ROLE	WT	ROLE	WT
Electrofluidmechanics						
Electrohydrodynamics						
Electrogasdynamics						
Flow Measurements						
Electrostatics						
Ions						
Fluid Mechanics						

Ib

A STUDY OF ION TRAJECTORIES IN POTENTIAL FLOWS

Michael R. Deluca

H. R. Velkoff

Interim Technical Report #11

Contract DA-31-124-ARO-D-246

July 1972

The Ohio State University Research Foundation
Columbus, Ohio 43212

FOREWORD

The work reported herein was sponsored in part by
the United States Army Research Office, Durham, under
Contract No. DA-31-124-ARO-D-246. The study presented
herein was conducted by Mr. Michael R. Deluca in ful-
filling the requirements for a thesis in his Master of
Science program at the Ohio State University.

ABSTRACT

An analytical investigation of the motion of ions in a
fluid was conducted to provide insight in the use of ions as
a fluid flow diagnostic tool. Assuming small space charge
density, potential fields and flows were considered. The
specific cases studied were fine corona wire to a circular
cylinder. Both steady and non-steady flows were considered
and the trajectories of the ions leaving the cornona wire
were mapped.

TABLE OF CONTENTS

LIST OF ILLUSTRATIONS

NOMENCLATURE

Symbol	Definition
a	"Pole", function of (r_1, r_2, S)
$\vec{a}_\eta$	Unit vector in η-direction
C_1	Lift coefficient
D	Diameter of cylinder
d_1	Distance from origin to wire
d_2	Distance from origin to cylinder
$\vec{E}$	Electric field strength
E_x	x-component of $\vec{E}$
E_y	y-component of $\vec{E}$
F_y	Lift force
f, g, h, i, k, ℓ	Functions
$f', g', h', i', k', \ell'$	Dimensionless functions
K	Ion mobility
K_0	Mobility at original conditions
M	Dimensionless parameter $\dfrac{K_0 V}{(\eta_2 - \eta_1) r_2 U}$
P	Pressure
P_0	Pressure at original conditions
r	Polar coordinate
r_1	Corona wire radius
r_2	Circular cylinder radius
S	Center spacing between wire and cylinder
S_T	Strouhal Number $\left(\dfrac{\omega D}{U}\right)$

Symbol	Definition
t	Time
t'	$\dfrac{tU}{D}$
U	Free stream velocity
V	Corona wire potential
$\vec{V}_D$	Drift velocity of ions
$\vec{V}_F$	Fluid velocity
$\vec{V}_I$	Ion velocity
V_{IX}	Ion velocity in x-direction
V_{IY}	Ion velocity in y-direction
W_F	Complex potential for fluid
x,y	Cartesian coordinates
$x',y',\ldots$	Dimensionless lengths $\left(x' = \dfrac{x}{r_2}, \ldots\right)$
α	Angles ions leave corona wire
γ	Angle ions intersect cylinder
ϵ	Permittivity
η	Bicylindrical coordinate
η_1	Value of η at corona wire
η_2	Value of η at cylinder
θ	Polar coordinate
θ_B	Bicylindrical coordinate
κ	Circulation
ξ	Vorticity
ρ	Fluid mass density
ρ_e	Electric charge density

Symbol	Definition
η_F	Potential for fluid
ψ_F	Stream function for fluid
ω	Circular frequency

I. INTRODUCTION

During the summer of 1968, Dr. Henry Velkoff of the Ohio State University performed experiments measuring the ion flow from a corona wire to a circular cylinder immersed in a fluid stream at varying Reynolds numbers. The experimental data shows oscillations in the ion flow (at approximately the Strouhal frequency) at certain locations on the cylinder and non-periodic variation of the current at other locations. The intent of the tests was to determine the efficacy of the "ion flow" technique for diagnosis of separation, transition, etc. The intent of this thesis is to analyze the same phenomenon from the standpoint of the ion trajectories.

II. STATEMENT OF PROBLEM

Consider a circular cylinder of radius (r_2) in a fluid stream of velocity (U). Directly upstream of the cylinder is a corona wire of radius (r_1), center spacing (S), and potential (V). The ions possess a mobility (K) and are leaving the corona wire at an angle (α) and intersecting the cylinder at an angle (γ). The problem is complicated by the unsteady behavior of the flow and the (possibly) varying mobility.
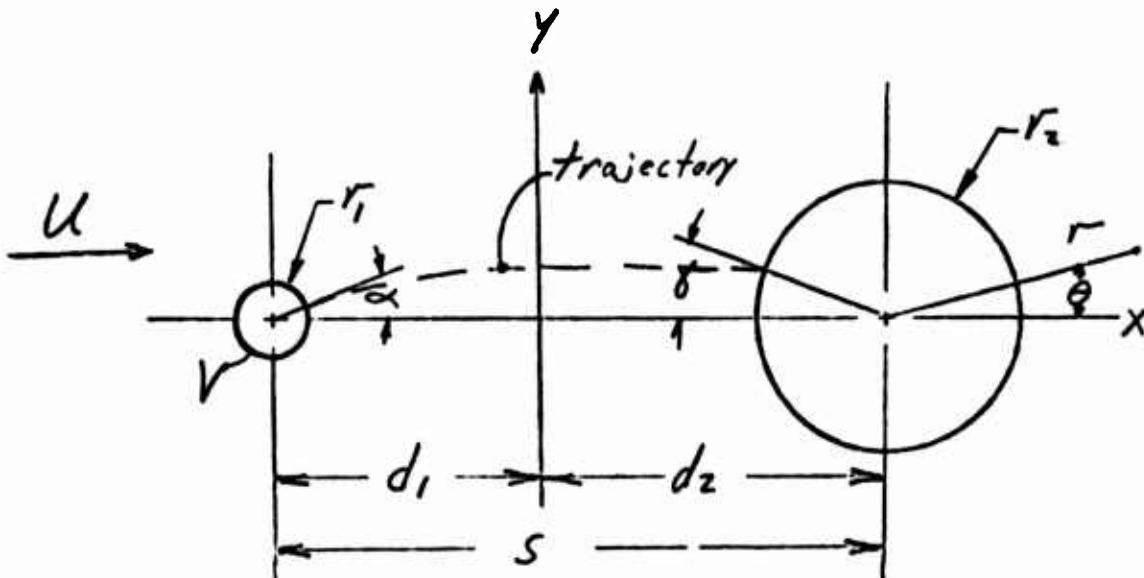

Figure 1 - Statement of Problem

1

This work will compute the ion trajectories, taking into consideration the unsteady nature of the flow and the variation in the mobility.

III. ANALYSIS

Corona Phenomena

Corona is the expression used to describe the class of luminous phenomena associated with the current jump at a highly stressed electrode preceding a spark breakdown of the gap. Associated with corona is an electrode of small radius. If such an electrode is placed near one of low curvature, the electric field induced is extremely high at the highly curved electrode. As the potential difference between the electrodes is raised, ionization of the air in the immediate vicinity of the highly curved electrode occurs; however, no spark crosses the gap because the field is too low farther from the curved electrode. The resulting corona discharge will be of positive or negative character depending upon the electrode polarity. If the highly curved electrode or wire has a negative potential, the positive ions formed near the wire acquire relatively high energy from the field and essentially bombard the cathode wire. These positive ions, while forming a space charge near the cathode which gives the negative corona its oscillating characteristic, will produce the necessary electrons to sustain the discharge. The electrons that are formed will travel relatively slowly to the anode because of the reduction in field strength away from the wire. These electrons will generally not have enough energy to cause further ionization and may be expected to attach themselves to neutral molecules of electro-negative gases forming large, even slower moving, ions. A wire of positive potential will attract the ionized electrons with great intensity causing electron avalanches toward the wire. This frees a positive ion space charge which moves toward the cathode sustaining the discharge although reducing the field at the wire. The space charge present in the region about a corona discharge causes a marked distortion of the electrostatic field (as Poisson's equation predicts). The fact that the highly ionized region constituting the corona envelope occupies only a very small volume near the wire permits the theoretical determination of the electric field from Laplace's equation rather than from Poisson's equation. (References 2, 8).

Electric Field Equations

Appendix B consists of an analysis of the electric field between two infinitely long conducting cylinders of different radii (r_1, r_2), center spacing (S) and electric potential difference (V). The results of this analysis (which assumed zero charge density) are

$$\vec{E} = - \vec{a\eta} \, \frac{V}{a(\eta_1 - \eta_2)} \, (\cosh \eta - \cos \theta_B)$$

$$E_x = - \frac{V}{(\eta_1 - \eta_2)} \, 2 \left| \frac{x(x^2+y^2-a^2)}{[(x^2+y^2-a^2)^2 + (2ay)^2]} - \frac{(x-a)}{[(x-a)^2 + y^2]} \right|$$

$$E_y = - \frac{V}{(\eta_1 - \eta_2)} \, 2y \left| \frac{x^2 + y^2 + a^2}{[(x^2+y^2-a^2)^2 + (2ay)^2]} - \frac{1}{[(x-a)^2 + y^2]} \right|$$

where

$$\eta = \ell n \, \frac{\sqrt{(x^2+y^2-a^2)^2 + (2ay)^2}}{(x-a)^2 + y^2}$$

$$\theta_B = - \tan^{-1} \frac{-2ay}{x^2 + y^2 - a^2}$$

$$\eta_1 = - \sinh^{-1} \left(\frac{a}{r_1} \right)$$

$$\eta_2 = \sinh^{-1} \left(\frac{a}{r_2} \right)$$

$$a = \frac{1}{2S} \left[S^4 - 2S \, (r_1^2 + r_2^2) + (r_2^2 - r_1^2)^{1/2} \right]$$

Also,

$$d_1 = (a^2 + r_1^2)^{1/2}$$

$$d_2 = (a^2 + r_2^2)^{1/2}$$

The geometrical significance of η and a is shown in Appendix E.

The corona wire will be ignored for the determination of the fluid velocity field. This is justifiable for two reasons: (1) the necessarily small diameter of the corona wire, (2) the high electric fields in the immediate vicinity of the wire dominates the movement of the ions in that region.

The diameter of the corona wire in most experiments ranges from .0015" to .004".

3

Flow Around a Circular Cylinder

The motion around a long circular cylinder immersed in a fluid stream is interesting for the variety of changes which occur with an increase in the Reynolds number. At a low Reynolds number the effects of viscosity are sensible at large distances from the cylinder, in particular the fluid at the back is retarded. At higher Reynolds numbers two symmetrical standing vortices are formed at the back. With increasing Reynolds numbers these vortices stretch farther and farther downstream from the cylinder. Eventually the standing vortices are drawn out to a considerable length, become distorted, and break down. Then develops the characteristic state of flow in which vortices are shed alternately and at regular intervals from the sides of the cylinder, with vortex trails behind: this type of flow persists over a large range of Reynolds numbers. The asymmetrical arrangement of the vortices alters the pressure distribution around the cylinder. The eddying motion has a definite frequency for each Reynolds number. Downstream the vortices assume what appears to be a regular pattern. The vortices arrange themselves in a double row, in which each vortex is opposite the mid-point of the interval between two vortices in the opposite row. In suitable circumstances the trail of vortices persists for a considerable distance downstream. The vortices actually do not arrange themselves exactly on two parallel rows with a definite spacing ratio. For theoretical purposes the system was considered by Von Karman to be composed of isolated vortices on two parallel rows. At higher Reynolds numbers the vortices diffuse so rapidly after their formation that it is no longer possible to speak of the formation of a double row. At the back of the cylinder, however, vortices continue to be shed with regularity until approximately Reynolds number $= 1.3 \times 10^5$. From Reynolds number $= 1.3 \times 10^5$ to 3.5×10^6 there is loss of the dominant periodicity (regularity) and there is a wide spectrum of frequencies to contend with. Above 3.5×10^6 recovery of the pronounced periodicity occurs. The range of Reynolds number 1.3×10^5 to 3.5×10^6 is called the "Critical" and "Post-Critical" regime. Above 3.5×10^6 the regime is termed "Transcritical." The classical description of the critical Reynolds number is (roughly): "At subcritical Reynolds numbers the separation is laminar, and occurs early, on the front of the cylinder. With increasing Reynolds number, transition to turbulence in the boundary layer moves ahead of the laminar separation point, the now turbulent boundary layer can withstand a greater pressure rise, and separation moves to the rear of the cylinder." Roshko postulates a new classification: "at subcritical Reynolds numbers the separation is laminar, in the supercritical range there is a laminar separation bubble followed by turbulent separation, and in the transcritical range the separation is purely turbulent. (References 4, 6, 10, 12)

It is well known that there acts on the cylinder an oscillatory lift force of the same order of magnitude of the mean drag and an oscillatory drag force superposed on the mean value. The oscillatory forces possess the same frequency as the shedding vortices (approximately).

Practically all the unsteady measurements in the broad subcritical range exhibit more or less randomly modulated signals at the Strouhal frequency whether they represent local values (e.g. local pressures on the cylinder) or integrated values (e.g. forces on short sections of the cylinder.) Figure 2 shows the results of experiments determining the root mean square oscillatory lift coefficient as a function of the Reynolds number. (References 4, 5, 10).

In the cases of the motion of water and air the Reynolds numbers are very large because of the very low viscosities of these fluids. It is reasonable to expect good agreement between experiment and a theory in which the influence of viscosity is neglected, i.e. with potential flow theory. The pressure distribution according to inviscid flow theory around a circular cylinder differs considerably from experiment depending on whether the Reynolds number lies in the range of subcritical or super-critical -- better agreement in the supercritical range. Experimental and calculated values show a measure of agreement on the front side, but at the rear of the cylinder the differences between experiment and theory are very large, and explain the large drag force experienced by a circular cylinder. The inviscid flow theory predicts zero drag. Although, gener-ally speaking, the theory of inviscid fluids does not give good results for drag calculations, the lift can be calculated from it successfully. (Reference 13).

It can be shown that if irrotational flow exists within some portion of fluid, then the circulation (κ), which is the line integral of the velocity vector taken around a closed curve within a fluid region, about any closed curve is zero and remains zero; and the permanence of irrota-tional flow is established. In the first instance, flow is irrotational. Due to the lack of slip at the boundaries, rotation starts here. Heat is imparted to a fluid from a body in the flow in exactly the same manner that vortices diffuse into the fluid. For very slow motion, i.e. low Reynolds numbers, heat flows out in all directions from the boundary, making the flow rotational. For high Reynolds numbers, the only fluid heated would be in the narrow layer of fluid surrounding the body and in the wake. Similarly, rotational flow is confined to the narrow layer adjacent to the boundary and to the wake. Therefore, the flow can be analyzed by considering the generation of unsteady vorticity in the prox-imity of the cylinder and the resulting feedback on the velocity and pressure fields near the cylinder. (References 10, 15).

Consider a cylinder shedding a Von Karman-like vortex trail (Figure 3). There is a time dependent amount of vorticity contained within the Curve C since vorticity in the wake is passing through the curve and the rate of generation of vorticity is also a function of time. For sub-critical and "transcritical" flow the vortex generation is accurately periodic. Consequently the amount of vorticity (ξ) enclosed in the curve can be represented mathematically by

$$\xi = \xi_0 \sin \omega t$$

5
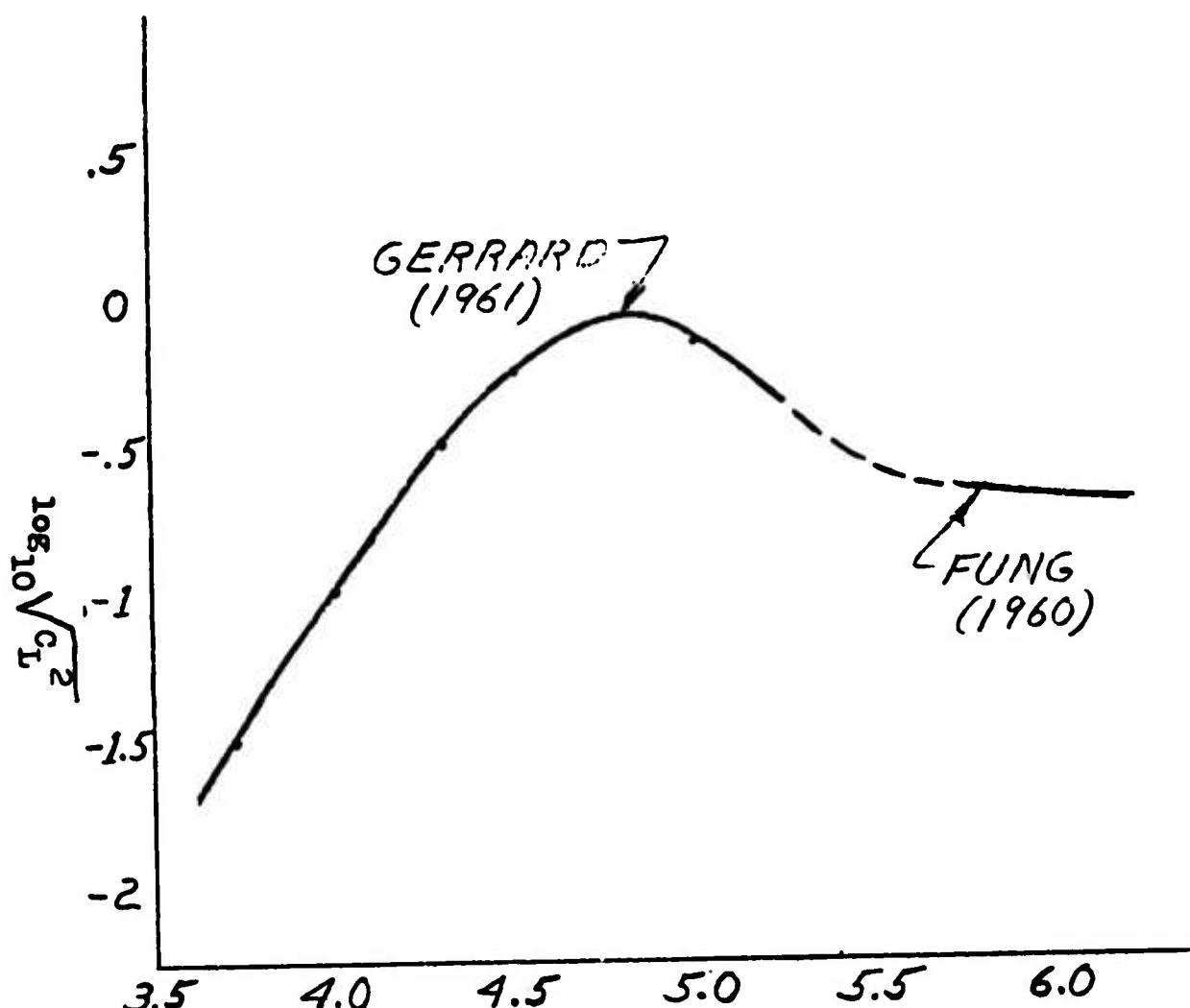
Figure 2 - Oscillating Lift Coefficient
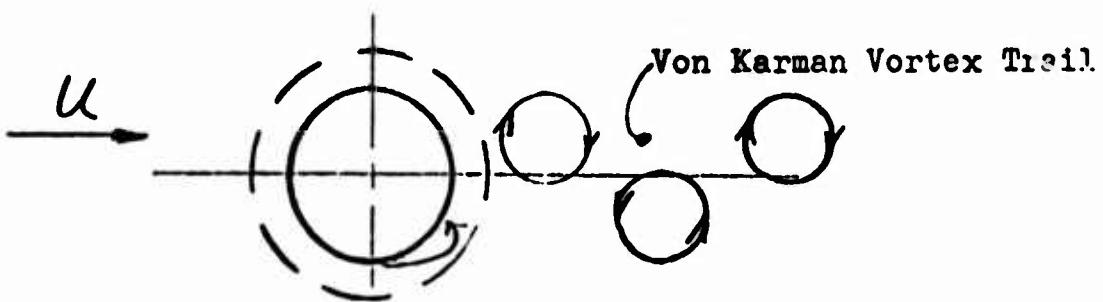
Figure 3 - Cylinder Shedding Vortices

where ξ_0 is the maximum vorticity of a single vortex and ω is the shedding frequency. The amount of circulation along the curve is proportional to the amount of vorticity, hence the circulation (κ) is

$$\kappa = \kappa_0 \sin \omega t$$

If we require the circulation about the curve to be zero, we must add $-\kappa$ to κ. This may be done by adding an isolated vortex at the center of the cylinder with a vorticity opposite to the vorticity generated at the cylinder wall. Superposing this isolated vortex to potential flow around the cylinder enables us to determine the feedback effect of the unsteady vorticity generated on the flow upstream of the cylinder.

Fluid Velocity Analysis

The complex potential $W_F = -Uz$ is for uniform flow with velocity U in the positive x-direction. The complex potential $W_F = -Ur^2/(z-zo)$ is for a doublet at point zo with axis in the x-direction. The superposition of the uniform flow upon the doublet yields steady flow around a circular cylinder. The complex potential $W_F = -(i\kappa/2\Pi)\ell n(z-zo)$ is for circulation κ about the point zo in the negative (clockwise direction). It can be shown that superposing this potential on the two previous potentials still represents flow around a circular cylinder. The total complex potential is then (Reference 15)

$$W_F = -Uz - \frac{Ur^2}{z-zo} - \frac{i\kappa}{2\Pi}\ell n\,(z-zo)$$

To correspond with the notation used in deriving the electric field strength components, we will call the radius of the cylinder (r_2) and the center ($zo = d_2$). Therefore

7

$$W_F = -U\left[z + \frac{r_2^2}{z-d_2}\right] - \frac{i\kappa}{2\pi} \ell n \ (z-d_2)$$

So

$$W_F = -U\left[x + iy + \frac{r_2^2}{x-d_2+iy}\right] - \frac{i\kappa}{2\pi} \ell n \ (x-d_2+iy)$$

Separating both sides of the equation into real and imaginary parts gives

$$\varphi_F = -U\left[x + r_2^2 \frac{x-d_2}{(x-d_2)^2+y^2}\right] + \frac{\kappa}{2\pi}\tan^{-1}\frac{y}{x-d^2}$$

The velocity components are computed by taking minus the gradient of the potential and are

$$V_{Fx} = -\frac{\partial\varphi F}{\partial x} = U\left[1 + r_2^2\frac{y^2-(x-d_2)^2}{[(x-d_2)^2+y^2]^2}\right] + \frac{\kappa}{2\pi}\left[\frac{y}{(x-d_2)^2+y^2}\right]$$

and

$$V_{Fy} = -\frac{\partial\varphi F}{\partial y} = -2Ur_2^2\left[\frac{y(x-d_2)}{(x-d_2)^2+y^2}\right] - \frac{\kappa}{2\pi}\left[\frac{x-d_2}{(x-d_2)^2+y^2}\right]$$

It will be found useful to have the velocity at the cylinder surface for later calculations of the lift force on the cylinder. Expressing z in polar coordinates, the complex potential is (for cylinder at origin)

$$W_F = -U\left(re^{i\theta} + \frac{r_2^2}{r}e^{-i\theta}\right) - \frac{i\kappa}{2\pi} \ell n \ (re^{i\theta})$$

which may be separated to yield

$$\varphi_F = -U\left(r + \frac{r_2^2}{r}\right)\cos\theta + \frac{\kappa}{2\pi}\theta$$

In polar coordinates the velocity components are V_r and V_θ. Obviously $V_r = 0$ at the cylinder. The total velocity consists of V_θ.

$$V_{F\theta} = -\frac{1}{r}\frac{\partial\varphi F}{\partial\varphi} = -U\left(1 + \frac{r_2^2}{r^2}\right) - \frac{\kappa}{2\pi}\frac{1}{r}$$

8

At the cylinder $r = r_2$. Hence,

$$V_{F\theta}\big)_{r = r_2} = -2U \sin \theta - \frac{\kappa}{2\pi r_2}$$

$$\left| \vec{V}_F \right|_{r = r_2} = 2U \sin \theta + \frac{\kappa}{2\pi r_2}$$

Ion Trajectory Analysis

The ions resulting from the high fields of the corona wire are transported from the wire by interaction with the neutral molecules of the fluid which flows with a velocity $\vec{V}_F(x,y,t)$. Uncharged molecules or ions with zero mobility will flow at a velocity of $\vec{V}_F$. The ions of one sign coming from the wire have associated with them a space charge field with an electric charge density $\rho_e(y,x)$ which modifies the electric field as:

$$\text{div}\vec{E}(x,y) = \rho_e(x,y)/\epsilon$$

Away from the wire we can assume (because of the extremely low charge density) that the space charge density is negligible and

$$\text{div}\vec{E}(x,y) = 0$$

The coupling between the fluid and the charges under the influence of the field gives rise to a drift velocity $\vec{V}_D(x,y)$ of the charges relative to the fluid.

$$\vec{V}_D(x,y) = K\vec{E}(x,y)$$

where K is the mobility of the ions. This expression (which is essentially the definition of mobility) comes from experimental results which have shown that the velocity of ions and electrons (in a dense gas) is proportional to the applied electric field. This is true as long as the energy gained by the ion is of the order of the thermal energy of gas.

The resulting transport velocity of the ions $\vec{V}_I(x,y,t)$ is as follows

$$\vec{V}_I(x,y,t) = \vec{V}_F(x,y,t) + \vec{V}_D(x,y)$$

9

or

$$\vec{V}_I(x,y,t) = \vec{V}_F(x,y,t) + K\vec{E}(x,y)$$

For increased pressure of the gas, the ion mobility decreases (over a large range of pressure) for constant temperature approximately as

$$K = K_o \frac{P_o}{P}$$

where the subscript (o) denotes the mobility and pressure at "original conditions." Therefore

$$\vec{V}_I(x,y,t) = \vec{V}_F(x,y,t) + \frac{P_o}{P} K_o \vec{E}(x,y)$$

Separating the velocity equation into the components in the x and y directions gives

$$V_{IX} = V_{FX} + \frac{P_o}{P} K_o E_x$$

$$V_{IY} = V_{FY} + \frac{P_o}{P} K_o E_y$$

The trajectories for the ion motion can be calculated from the differential equation that results from taking the ratio of the velocity components.

$$\frac{V_{IY}}{V_{IX}} = \frac{\dfrac{dy}{dt}}{\dfrac{dx}{dt}} = \frac{dy}{dx} = \frac{V_{FY} + \dfrac{P_o}{P} K_o E_y}{V_{FX} + \dfrac{P_o}{P} K_o E_x}$$

The solution of this trajectory equation for steady and unsteady flow, constant and variable mobility, and for a wide range of the system parameters (as will be determined from the dimensionless-sizing of the differential equation) constitutes the remainder of this thesis.

Let

$$x' = \frac{x}{r_2}, \quad y' = \frac{y}{r_2}, \quad s' = \frac{s}{r_2}, \quad a' = \frac{a}{r_2}, \quad \text{etc.}$$

Then the fluid velocity and electric field components are written

$$V_{FX} = U \left\{ 1 + \frac{y'^2 - (x'-d_2')^2}{(x'-d_2')^2 + y'^2} \right\} + \frac{\kappa}{2\pi r_2} \left[\frac{y'}{(x'-d_2')^2 + y'^2} \right]$$

10

$$V_{FY} = -2U \left\{ \frac{y'(x'-d_2')}{(x'-d_2')^2 + y'^2} \right\} - \frac{\kappa}{2\pi r_2} \left[\frac{x'-d_2'}{(x'-d_2')^2 + y'^2} \right]$$

$$E_x = \frac{V}{(\eta_2-\eta_1)r_2} \cdot 2 \left\{ \frac{x'(x'^2+y'^2-a'^2)}{(x'^2+y'^2-a'^2)^2 + (2a'y')^2} - \frac{x'-a'}{(x'-a')^2 + y'^2} \right\}$$

$$E_y = \frac{V}{(\eta_2-\eta_1)r_2} \cdot 2y \left\{ \frac{x'^2+y'^2+a'^2}{(x'^2+y'^2-a'^2)^2 + (2a'y')^2} - \frac{1}{(x'-a')^2 + y'^2} \right\}$$

The above equations may be written

$$V_{FX} = U \cdot f(x',y',d_2') + \frac{\kappa}{r_2} \cdot g(x',y',d_2')$$

$$V_{FY} = U \cdot h(x',y',d_2') + \frac{\kappa}{r_2} \cdot j(x',y',d_2')$$

$$E_x = \frac{V}{(\eta_2-\eta_1)r_2} \cdot K(x',y',a')$$

$$E_y = \frac{V}{(\eta_2-\eta_1)r_2} \cdot \ell(x',y',a')$$

In general the pole a is

$$a = \frac{1}{2S} \left[S^4 - 2S^2(r_1^2 + r_2^2) + (r_2^2 - r_1^2)^2 \right]^{1/2}$$

For $r_1 < r_2$, this pole becomes

$$a = \frac{1}{2S} \left[S^2 - r_2^2 \right]$$

Also, in general, the distance from the origin to the center of the cylinder is

$$d_2 = S - d_1 = S - (a^2 + r_1^2)^{1/2}$$

So, since a is of the order of V:

$$d_2 = S - a = S - \frac{1}{2S}(S^2 - r_2^2)$$

which becomes

$$d_2 = \frac{1}{2S} \left[S^2 + r_2^2 \right]$$

11

In the primed coordinates the expressions for the pole a' and d_2' are

$$a' = \frac{1}{2S'} [S'^2 - 1]$$

$$d_2' = \frac{1}{2S'} [S'^2 + 1]$$

Therefore a' and d_2' are functions solely of the ratio of center distance to cylinder radius. Therefore the fluid velocities (that are a function of the space coordinates and d_2'), and the electric field strength (which is a function of the space coordinates and a') are all functions only of (besides U, V, r_2, K, $(\eta_1 - \eta_2)$ the space coordinates and the ratio of the center distance to the cylinder radius (S'). So

$$V_{FX} = U \cdot f'(x',y',S') + \frac{K}{r_2} \cdot g'(x',y',s')$$

$$V_{FY} = U \cdot h'(x',y',s') + \frac{K}{r_2} \cdot j'(x',y',s')$$

$$E_X = \frac{V}{(\eta_2 - \eta_1)r_2} \cdot K'(x',y',s')$$

$$E_Y = \frac{V}{(\eta_2 - \eta_1)r_2} \cdot \ell'(x',y',s')$$

To fully understand the effects of the nonsteady circulation and variable mobility on the ion trajectory, three separate cases will be studied: (1) zero circulation, constant mobility; (2) unsteady circulation, constant mobility; and (3) zero circulation, variable mobility. Three separate cases lead to different but similar trajectory differential equations.

For case (1) the trajectory equation becomes

$$\frac{dy}{dx} = \frac{dy'}{dx'} = \frac{U \cdot h' + \frac{K_0 V}{(\eta_2 - \eta_1)r_2} \cdot \ell'}{U \cdot f' + \frac{K_0 V}{(\eta_2 - \eta_1)r_2} \cdot K'}$$

12

Dividing the numerator and denominator by the free stream velocity (U) gives

$$\frac{dy'}{dx'} = \frac{h' + \dfrac{K_0 V}{(\eta_2 - \eta_1) r_2 U} \cdot \ell'}{f' + \dfrac{K_0 V}{(\eta_2 - \eta_1) r_2 U} \cdot K'}$$

Therefore trajectories for this case are controlled by the two parameters

$$S', \quad \frac{K_0 V}{(\eta_2 - \eta_1) r_2 U}$$

Henceforth the second of these parameters will be designated (M)

$$M \equiv \frac{K_0 V}{(\eta_2 - \eta_1) r_2 U}$$

For case (2) the equation becomes

$$\frac{dy'}{dx'} = \frac{h' + \dfrac{K_0}{r_2 U} \sin \omega t \cdot j' + M \cdot \ell'}{f' + \dfrac{K_0}{r_2 U} \sin \omega t \cdot g' + M \cdot K'}$$

Since the time appears in the trajectory equation case (2) becomes the problem of solving simultaneous differential... equations, the trajectory equation being one and either

$$\frac{dx}{dt} = U \cdot f' + \frac{K_0}{r_2} \sin \omega t \cdot g' + \frac{K_0 V}{(\eta_2 - \eta_1) r_2} \cdot K'$$

or

$$\frac{dy}{dt} = U \cdot h' + \frac{K_0}{r_2} \sin \omega t \cdot j' + \frac{K_0 V}{(\eta_2 - \eta_1) r_2} \cdot \ell'$$

being the other equation. Let

$$t' = \frac{tU}{2r_2} = \frac{tU}{D}$$

13

This leads to

$$\frac{1}{2} \frac{dx'}{dt'} = f' + \frac{\kappa_O}{r_2 U} \sin\left(\frac{\omega D}{U} t'\right) \cdot g' + M \cdot K'$$

and

$$\frac{1}{2} \frac{dy'}{dt'} = h' + \frac{\kappa_O}{r_2 U} \sin\left(\frac{\omega D}{U} t'\right) \cdot j' + M \cdot \ell'$$

As stated previously ω is the shedding frequency.

Therefore

$$\frac{\omega D}{U} = 2\pi S_T$$

where S_T is the Strouhal number. So

$$\frac{1}{2} \frac{dx'}{dt'} = f' + \frac{\kappa_O}{r_2 U} \sin(2\pi S_T t') + M \cdot K'$$

and

$$\frac{1}{2} \frac{dy'}{dt'} = h' + \frac{\kappa_O}{r_2 U} \sin(2\pi S_T t') \cdot j' + M \cdot \ell'$$

Consequently case (2) has four parameters

$$S', \quad M, \quad \frac{\kappa_O}{r_2 U}, \quad S_T$$

Finally case (3) has the equation

$$\frac{dy'}{dx'} = \frac{h' + \frac{P_O}{P} M \cdot \ell'}{f' + \frac{P_O}{P} M \cdot K'}$$

We must now determine the pressure ratio. For an incompressible, steady flow, the Bernoulli equation is (reference 15)

$$\frac{1}{2} \rho V_F^2 + P = \frac{1}{2} \rho U^2 + P_O$$

Therefore

$$\frac{P}{P_O} = 1 - \frac{1}{2} \frac{\rho}{P_O} (U^2 - V_F^2)$$

14

So

$$\frac{P}{P_0} = 1 - \frac{1}{2}\frac{\rho}{P_0}U^2(1-f'^2-h'^2)$$

Hence, the trajectory equation becomes

$$\frac{dy'}{dx'} = \frac{h' + \dfrac{M}{1 - \dfrac{1}{2}\dfrac{\rho U^2}{P_0}(1-f'^2-h'^2)} \cdot \ell'}{f' + \dfrac{M}{1 - \dfrac{1}{2}\dfrac{\rho U^2}{P_0}(1-f'^2-h'^2)} \cdot \ell'}$$

And the variable mobility case is controlled by the three parameters

$$S', \quad M, \quad \frac{1}{2}\frac{\rho U^2}{P_0}$$

Case (1) and (3) are ready for solution now, but case (2) requires a determination of the proper amount of circulation for which to solve the equations. As stated previously inviscid flow theory has been relatively successful at calculating the lift on bodies immersed in a viscous fluid stream. For steady circulation, the lift force is directly proportional to the amount of circulation (Streeter). Morkovin, Gerrard and Fung all summarize their own and other experiments which determined the lift coefficient (oscillating) on a circular cylinder. It thus seems reasonable to attempt to find the proper amount of circulation from an integration of the pressure about the cylinder and the relation of this value to the experimentally determined lift coefficients. For nonsteady, incompressible flow, Bernoulli's equation is (Reference 15)

$$V_F{}^2 - \frac{\partial \varphi F}{\partial t} + \frac{P}{\rho} = F(t)$$

where $F(t)$ is an arbitrary function of time. We desire to find the lift force by integrating at the cylinder, therefore

$$V_F = 2U\sin\theta + \frac{\kappa}{2\pi r_2}$$

and

$$\varphi_F = -2Ur_2\cos\varphi + \frac{\kappa}{2\pi}\theta$$

$$\varphi_F = -2Ur_2\cos\theta + \frac{\theta}{2\pi}\kappa_0\sin\omega t$$

15

Hence,

$$\frac{\partial \varphi F}{\partial t} = \frac{\theta}{2\pi} \kappa_0 \, \omega \cos \omega t$$

Therefore,

$$P = \rho \left[F(t) + \frac{\kappa_0 \omega}{2\pi}(\cos \omega t)\theta - \frac{1}{2}\left(2U \sin \theta + \frac{\kappa_0}{2\pi r_2} \sin \omega t\right)^2 \right]$$

The force in the y direction is

$$F_y = \int_0^{2\pi} P \, r_2 \, d\theta \, \sin \theta$$

Substituting the pressure (P) into the integral gives

$$F_y = \rho U \kappa_0 \, \sin \omega t + \rho r_2 \omega \kappa_0 \cos \omega t$$

which can be written

$$F_y = \rho \kappa_0 \sqrt{U^2 + (r_2 \omega)^2} \left[\sin(\omega t + \gamma) \right]$$

$$\gamma = \tan^{-1} \frac{U}{\gamma_2 \omega}$$

Again,

$$\omega = 2\pi S_T \frac{U}{D} = \pi S_T \frac{U}{r_2}$$

So

$$\left| F_y \right| = \rho \kappa_0 \sqrt{U^2 + r_2^2 \left(\frac{\pi S_T U}{r_2}\right)^2}$$

and

$$\left| F_y \right| = \rho \kappa_0 U \sqrt{1 + (\pi S_T)^2}$$

Which is interesting because of the dependence of the oxcillating lift force on the Strouhal number. However κ_0 is an unknown quantity and no conclusions can be made regarding the variation of the lift force with the Strouhal number.

The lift coefficient is defined by

$$C_L = \frac{F_y}{\frac{1}{2}\rho U^2 D}$$

16

Substituting,

$$C_L = \frac{\rho \kappa_0 U \sqrt{1 + (\pi S_T)^2}}{\frac{1}{2}\rho U^2 2 r_2}$$

Hence

$$\frac{\kappa_0}{r_2 U} = \frac{C_L}{\sqrt{1 + (\pi S_T)^2}}$$

where $\left(\dfrac{\kappa_0}{r_2 U}\right)$ is exactly the dimensionless parameter found for case (2)!

Since C_L and S_T are known for a wide range of Reynolds numbers, the equivalent amount of circulation required can be calculated.

A calculation of the <u>drag</u> force for the assumed oscillating circulation showed this force to again be zero.

The corona wire was neglected in the fluid velocity analysis because of the small diameter and high electric field associated with the corona effect. It is now possible to determine approximately <u>what</u> radius wire is required for this assumption to be valid.

From potential theory, the maximum fluid velocity about any circular cylinder occurs at the "shoulder" and is twice the free stream velocity.

If we require that this maximum fluid velocity is less than one percent of the drift velocity caused by the action of the electric field on the ion, we have a means of calculating r_1.

$$\left|\vec{V_F}\right|_{max} = 2U, \quad \vec{V_D} = K\left|\vec{E}\right|$$

Therefore

$$\frac{\left|\vec{V_F}\right|_{max}}{\left|\vec{V_D}\right|} = \frac{2U}{K\left|\vec{E}\right|} < 0.01$$

$$\vec{E} = \frac{a'_\eta V}{a(\eta_2 - \eta_1)} (\cos h\eta - \cos\theta_B)$$

and

$$\eta = \sinh^{-1}\left(\frac{a}{r}\right) = \ell n\left[\frac{a}{r} + \left(\frac{a^2}{r^2} + 1\right)^{1/2}\right]$$

17

Hence for γ_1 small, i.e. $r_1 << a$.

$$\eta_1 = \ell n \left(\frac{2a}{r_1} \right)$$

and

$$\text{Cosh}\eta_1 = \frac{1}{2} \left(e^{\eta_1} + e^{-\eta_1} \right) = \frac{a}{r_1}$$

So we can neglect the $\cos \theta$ term in the field strength equation. Therefore

$$\left| \vec{E} \right| = \frac{V}{(\eta_2 - \eta_1) r_1}$$

So

$$\frac{\left| \vec{V}_F \right|}{\left| \vec{V}_D \right|} = \frac{2U}{K \dfrac{V}{(\eta_2 - \eta_1) r_1}} = \frac{2U r_2 (\eta_2 - \eta_1)}{KV} \left(\frac{r_1}{r_2} \right)$$

Or

$$\frac{r_1}{r_2} < .01 \frac{KV}{2 r_2 (\eta_2 - \eta_1) U} = .005 \, M$$

It was determined that a suitable minimum (for a typical experiment) for M is 1/8. Therefore

$$r_1{}' = \frac{r_1}{r_2} \leq 6.25 \, (10^{-4})$$

In Dr. Velkoff's experiment, the diameter of the corona wire was .0015", the diameter of the cylinder was 6". This yields an $r_1{}'$ of $2.5(10^{-4})$ which satisfies the criteria.

18

IV. DISCUSSION OF RESULTS

For case (1), zero circulation and constant mobility, it was decided to consider three values of S' (1.5, 2, 3), (Dr. Velkoff's experiment used 1.5), and three values of M (2, 0.5, 0.125), (Dr. Velkoff's experiment M was approximately 0.7). The ion trajectories (streamlines) for this case are represented in Figures 4 through 12. The most striking feature of these curves is the fact that although the trajectories of the ions are greatly altered by variation in the parameter M, the point at which the trajectories intersect the large cylinder is not changed very much. This indicates that for a fixed S' (Corona wire spacing), the average current reaching the large cylinder does not vary significantly with M. Since the variation in M could represent a 16-fold increase in the free stream velocity this is a significant fact. The current distribution along the cylinder was calculated by assuming that the current density around the corona wire was uniform. Therefore the current density at the cylinder would be proportioned to the ratio of the angle at which the ion leaves the corona wire to the angle at which the ion "collides" with the cylinder. So

$$J\left[\gamma_n + \frac{1}{2}(\gamma_{n+1} - \gamma_n)\right] = \frac{\alpha_{n+1} - \alpha_n}{\gamma_{n+1} - \gamma_n}$$

Where n denotes the trajectory number, J is a dimensionless number proportional to the current density, α is the angle at which the ions depart the corona wire, and γ is the angle at which the ions intersect the cylinder. Figure 13 through 16 are the results of this calculation and show clearly the small effect the variation in M has on the average currents and the relatively large effect the variation in the parameter S' has on the average current. Indeed, there is only a 14 percent change in the maximum current (at the stagnation point) for the 1600 percent change in M. Of course, the corona phenomenon must be considered. Since M is directly proportional to the applied voltage, an M variation due to voltage variation would undoubtedly produce a different number of ions at the corona wire and a subsequent change in the absolute value of the currents at the cylinder. Hence the shape of the current of Figure 13 through 16 are their only distinguishing feature for voltage variations. These curves indicate the currents at the front of the cylinder would decrease with a rising free stream velocity. This contradicts the experimental evidence from Dr. Velkoff's work. The data from his experiment showed an increase in the stagnation point current for an increase in free stream velocity. Dr. Velkoff's experiment included "field shaping" electrodes at ground potential in the vicinity of the corona wire which may account for the difference. Possibly the higher drag on the corona wire caused a deflection toward the cylinder which increased the current. A rough calculation showed a deflection of 0.125 inch would be required to account for the rise in current measured. This amount of deflection is unlikely. Another possible cause of the

19

Fluid stream

Circular cylinder

Corona wire

Ions leaving corona wire at angles ($\propto$) of 30°, 60°, 90°, 120°, 150°.
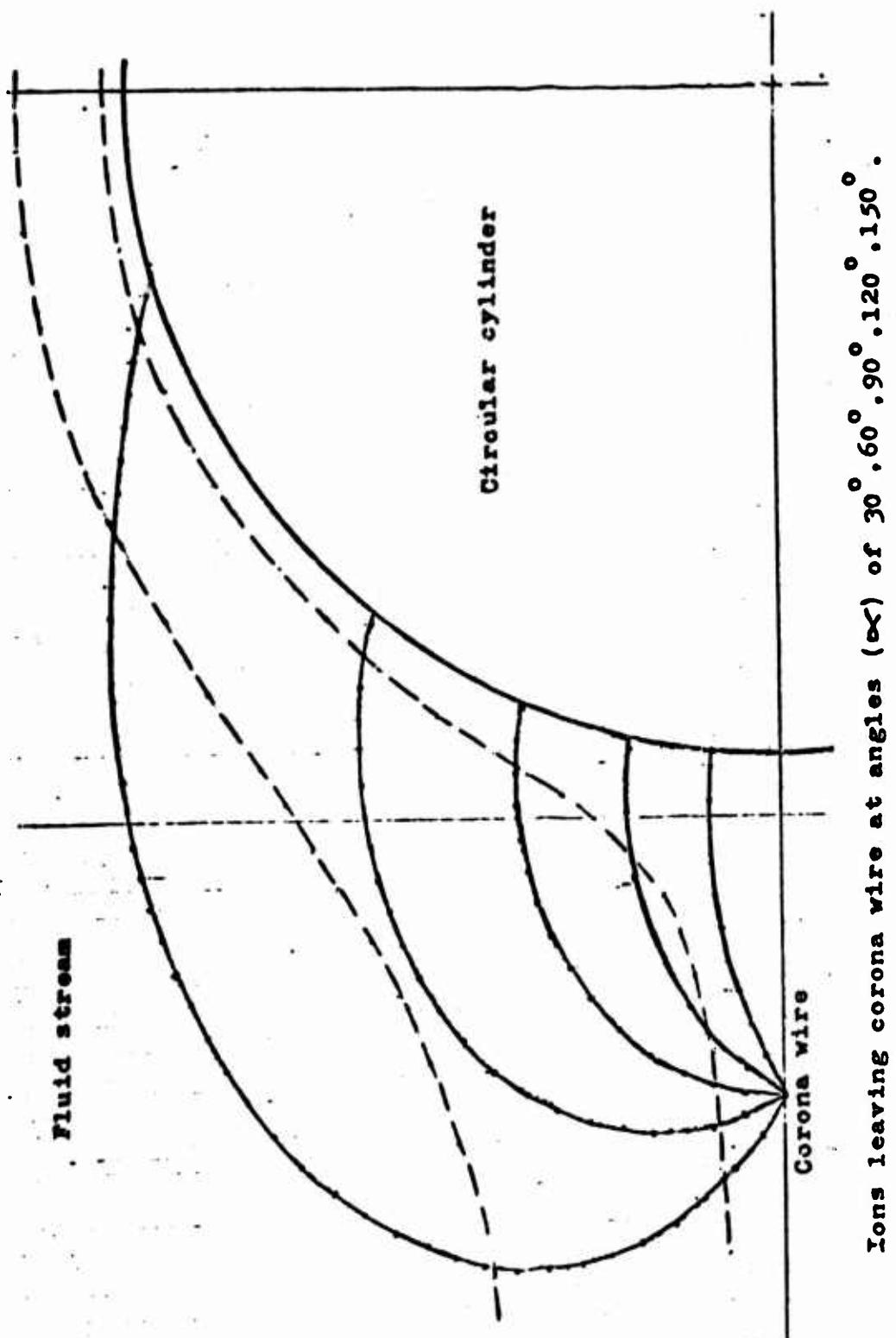
Figure 4. Ion Trajectories for M = 2, S' = 1.5.
(Dashed Lines - Fluid Streamlines, Solid Lines - Ion Trajectories).

20
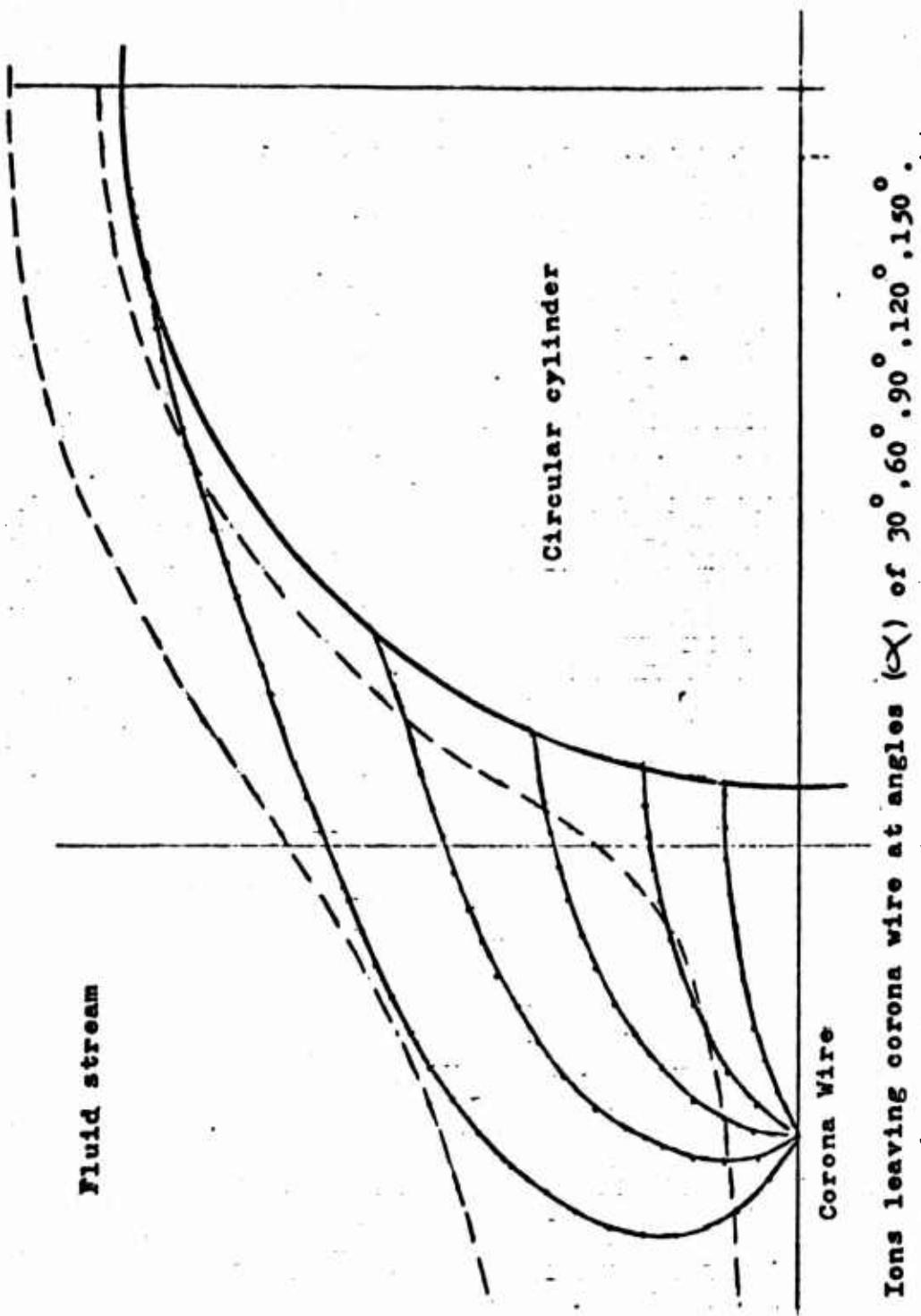
Figure 5. Ion Trajectories for M = 0.5, S' = 1.5.
(Dashed Lines-Fluid Streamlines, Solid Lines-Ion Trajectories)

Ions leaving corona wire at angles ($\propto$) of 30°, 60°, 90°, 120°, 150°.

Corona Wire

Circular cylinder
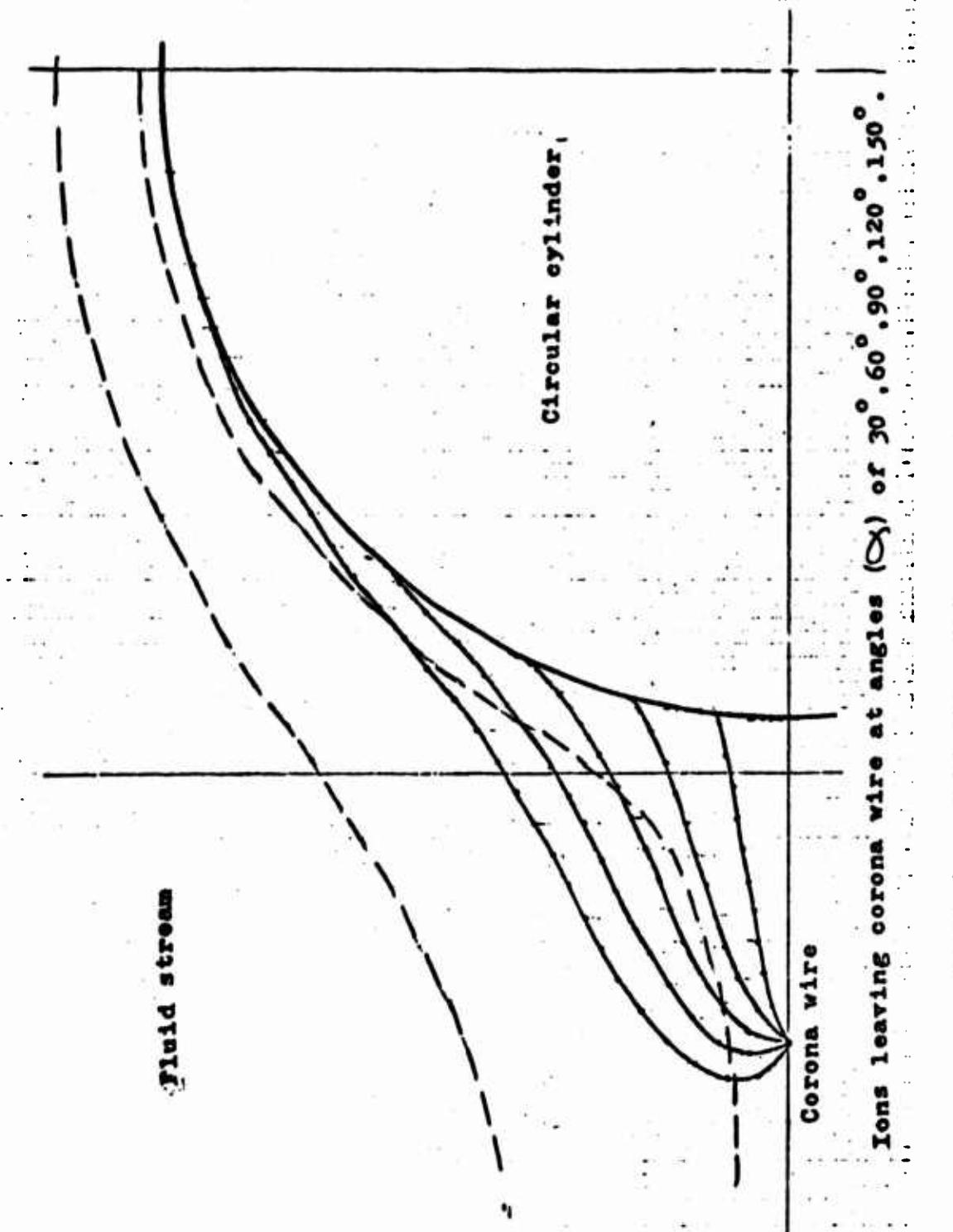
Fluid stream

Figure 6. Ion Trajectories for M = 0.125, S' = 1.5.
(Dashed Lines-Fluid Streamlines, Solid Lines-Ion Trajectories)

22

Fluid stream

Circular cylinder

Corona wire

Ions leaving corona wire at angles (α) of 30°, 60°, 90°, 120°, 150°.
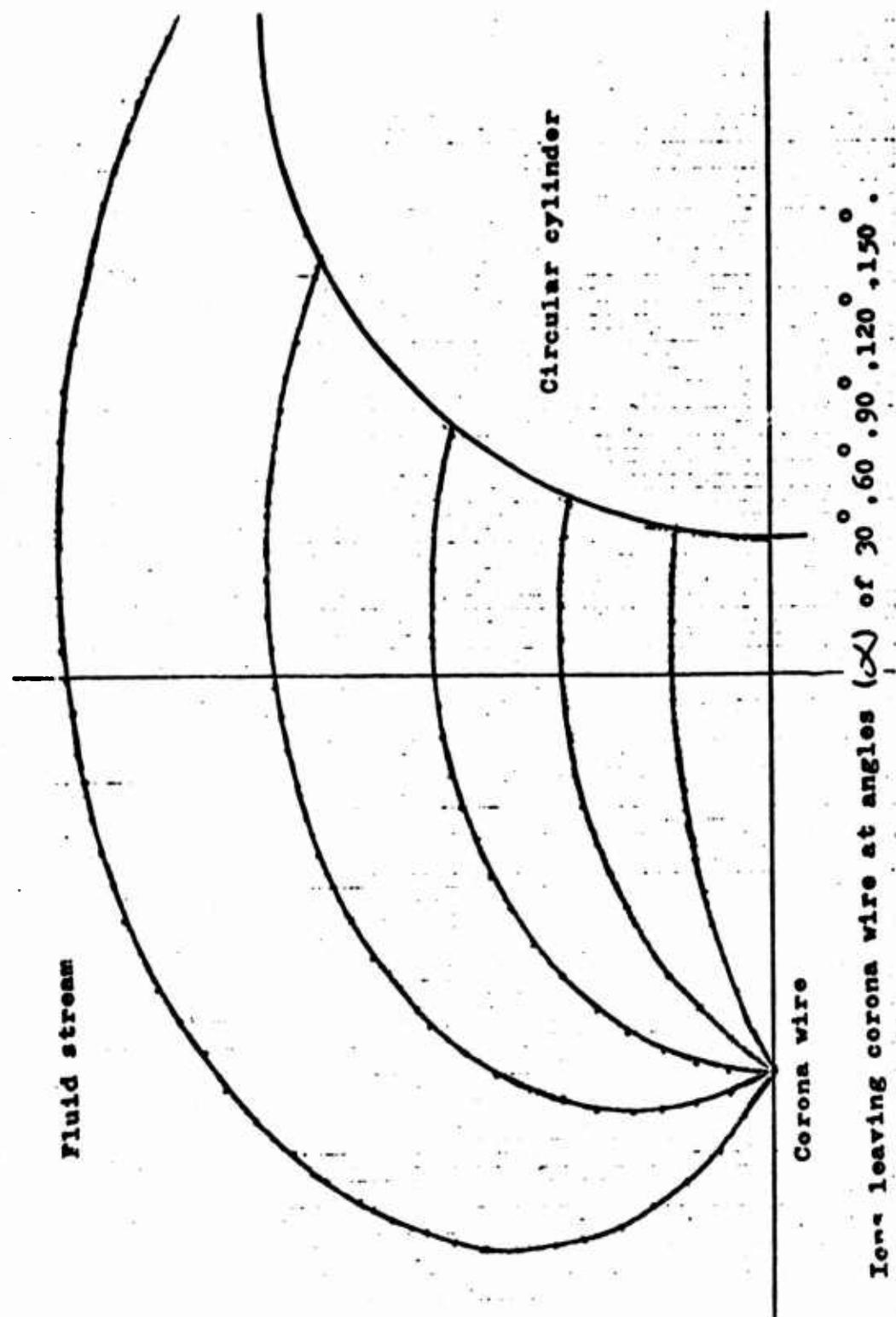
Figure 7. Ion Trajectories for M = 2, S' = 2.

23
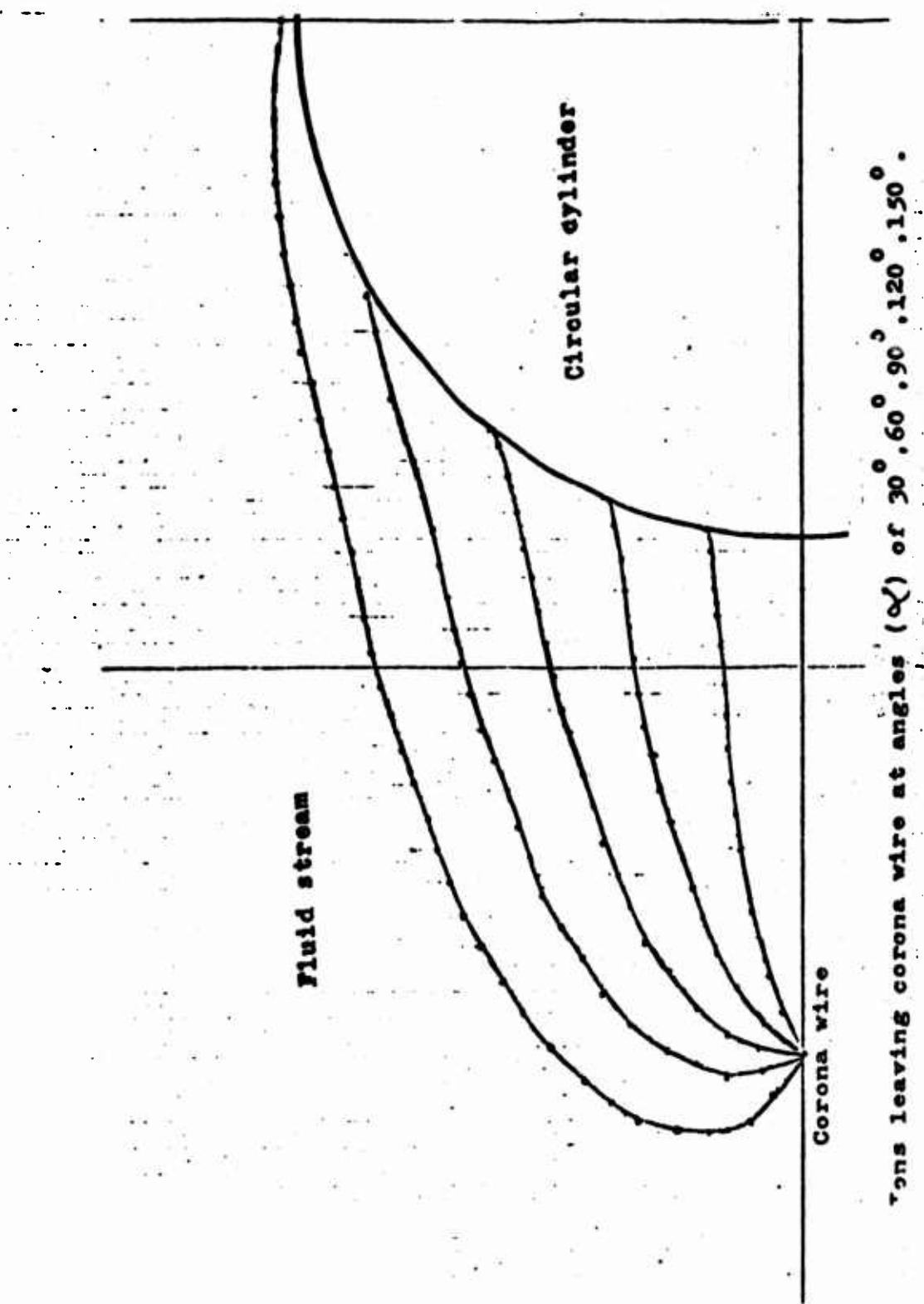
Figure 8. Ion Trajectories for M = 0.5, S' = 2.

Ions leaving corona wire at angles (α) of $30°, 60°, 90°, 120°, 150°$.
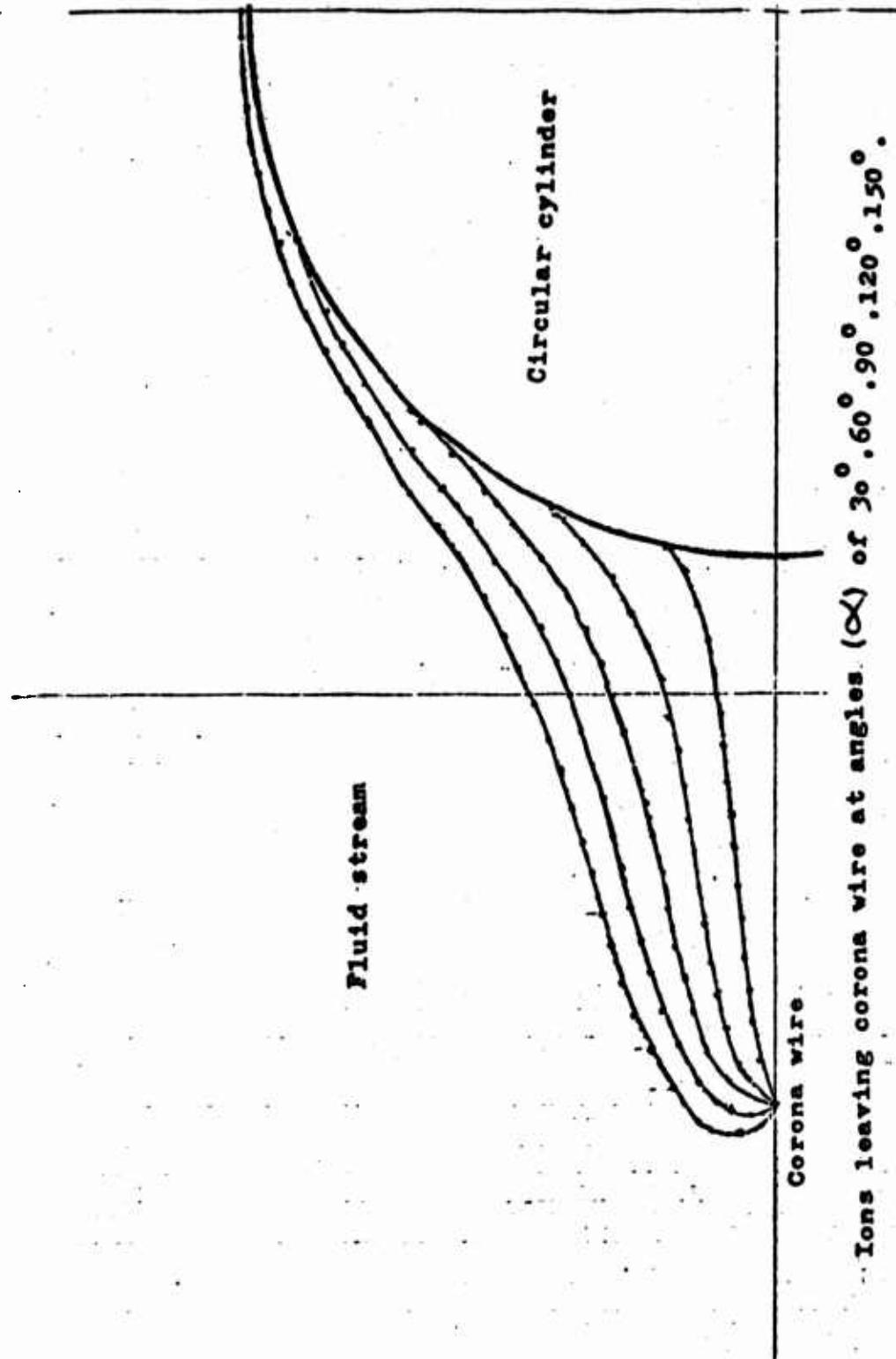
Figure 9. Ion Trajectories for M = 0.125, S' = 2.

Ions leaving corona wire at angles (α) of 30°,60°,90°,120°,150°.

Circular cylinder

Fluid stream

Corona wire
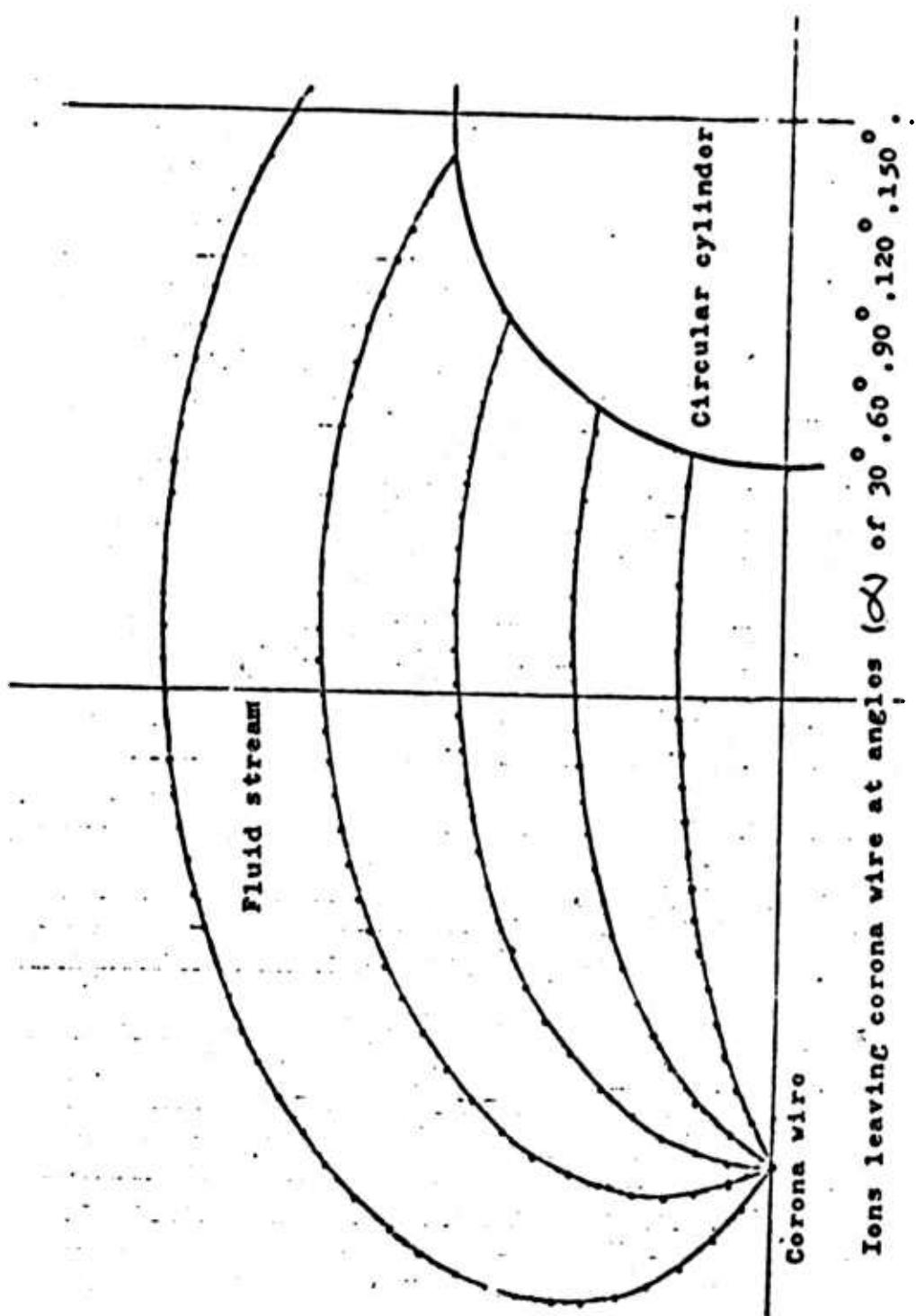
Figure 10. Ion Trajectories for $M = 2.0$, $S' = 3$.

26

Ions leaving corona wire at angles (α) of $30°$, $60°$, $90°$, $120°$, $150°$.
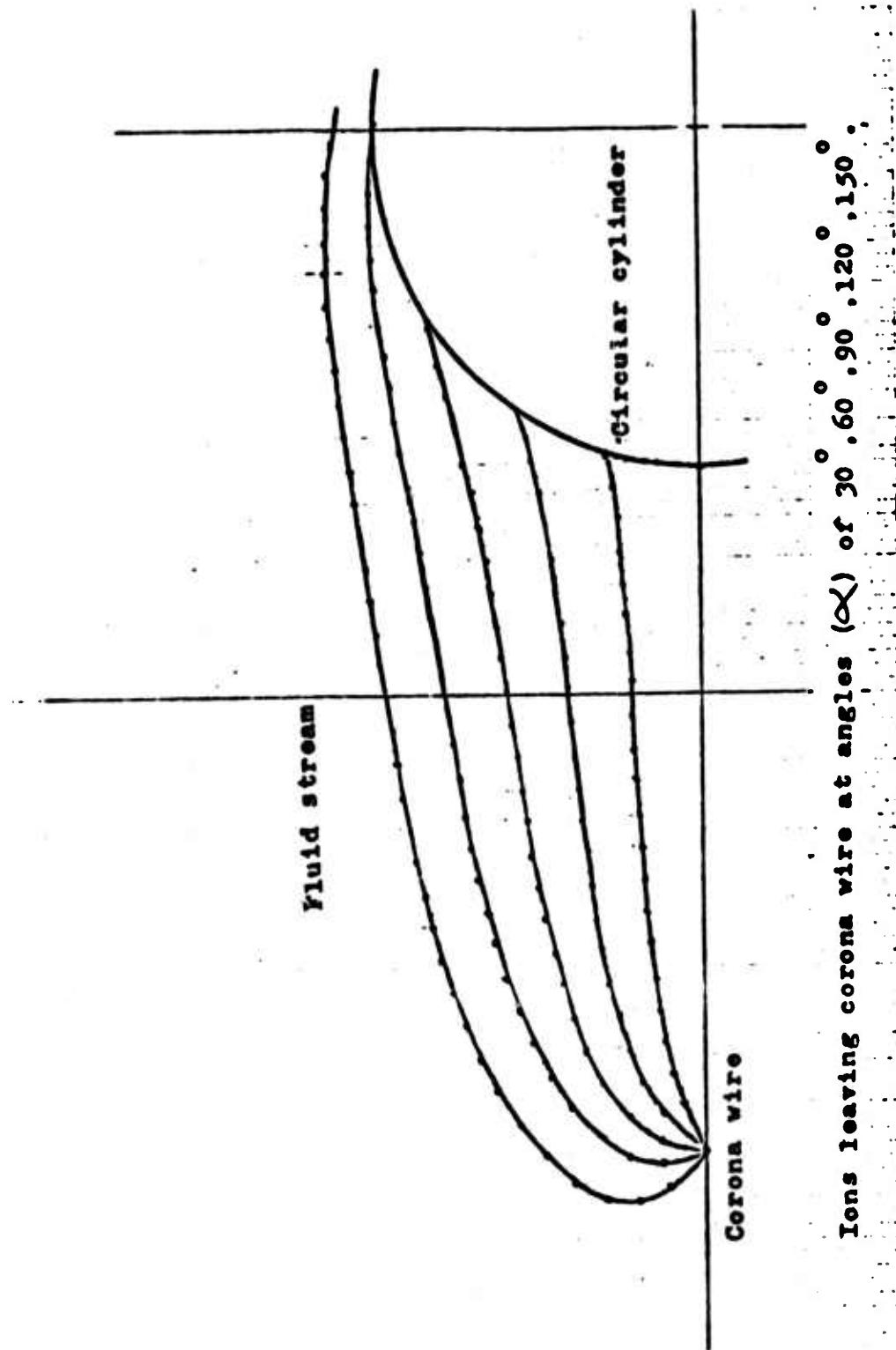
Figure 11. Ion Trajectories for M = .5, S' = 3.

27

Circular cylinder

Fluid stream

Corona wire

Ions leaving corona wire at angles (α) of 30°, 60°, 90°, 120°, 150°.
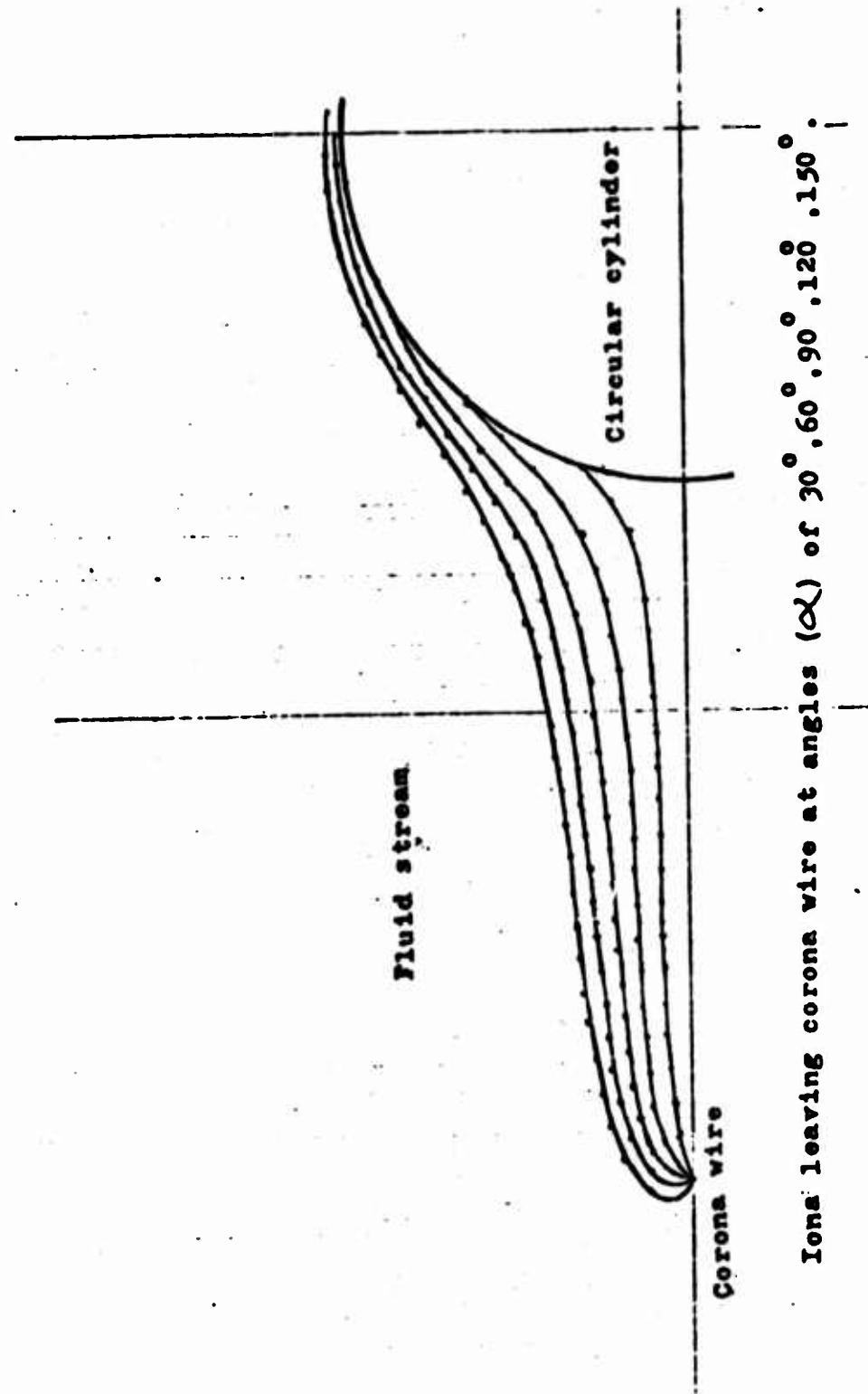
Figure 12. Ion Trajectories for M = .125, S' = 3.

26
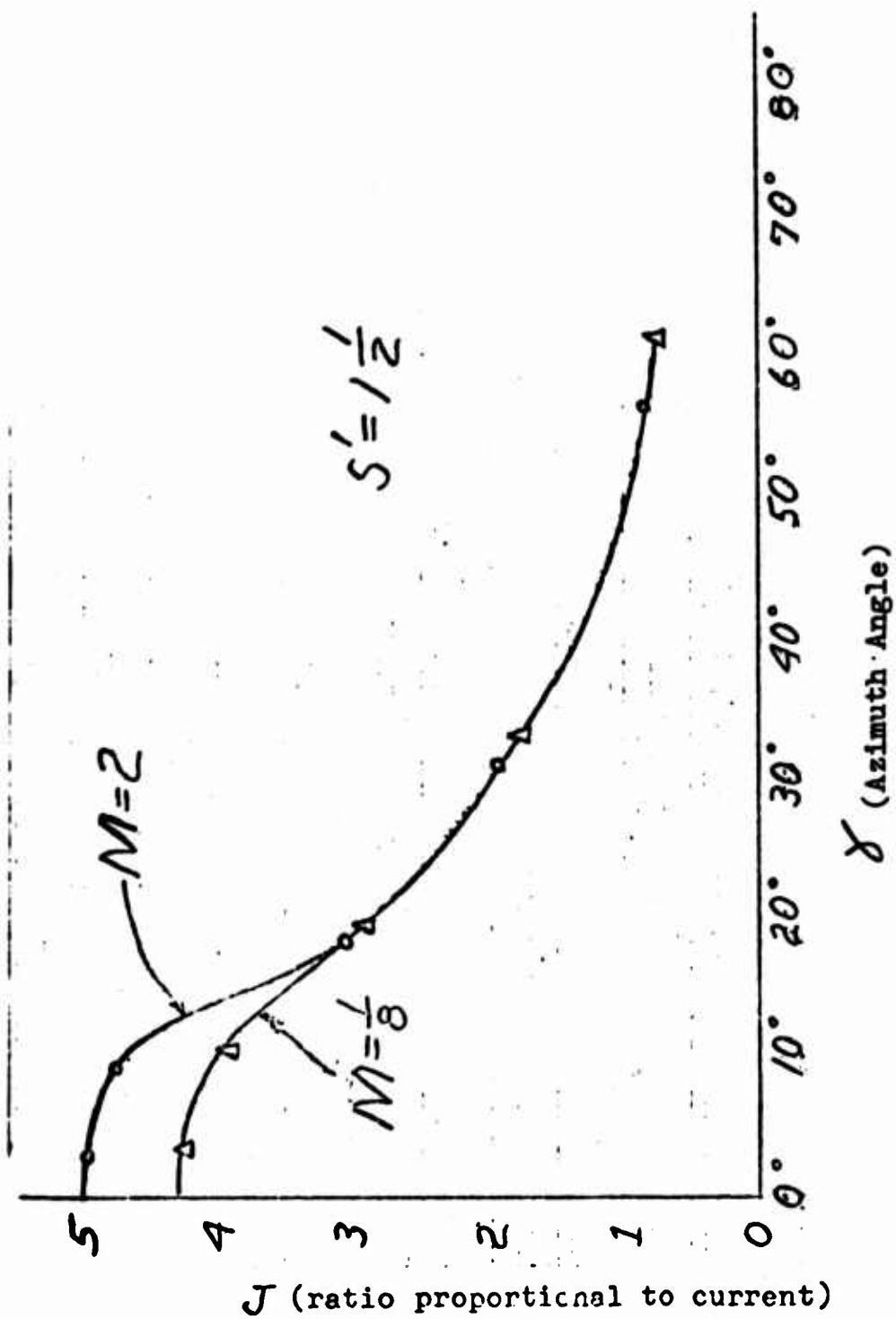
Figure 13. Current Distribution Around Cylinder for S' = 1.5.
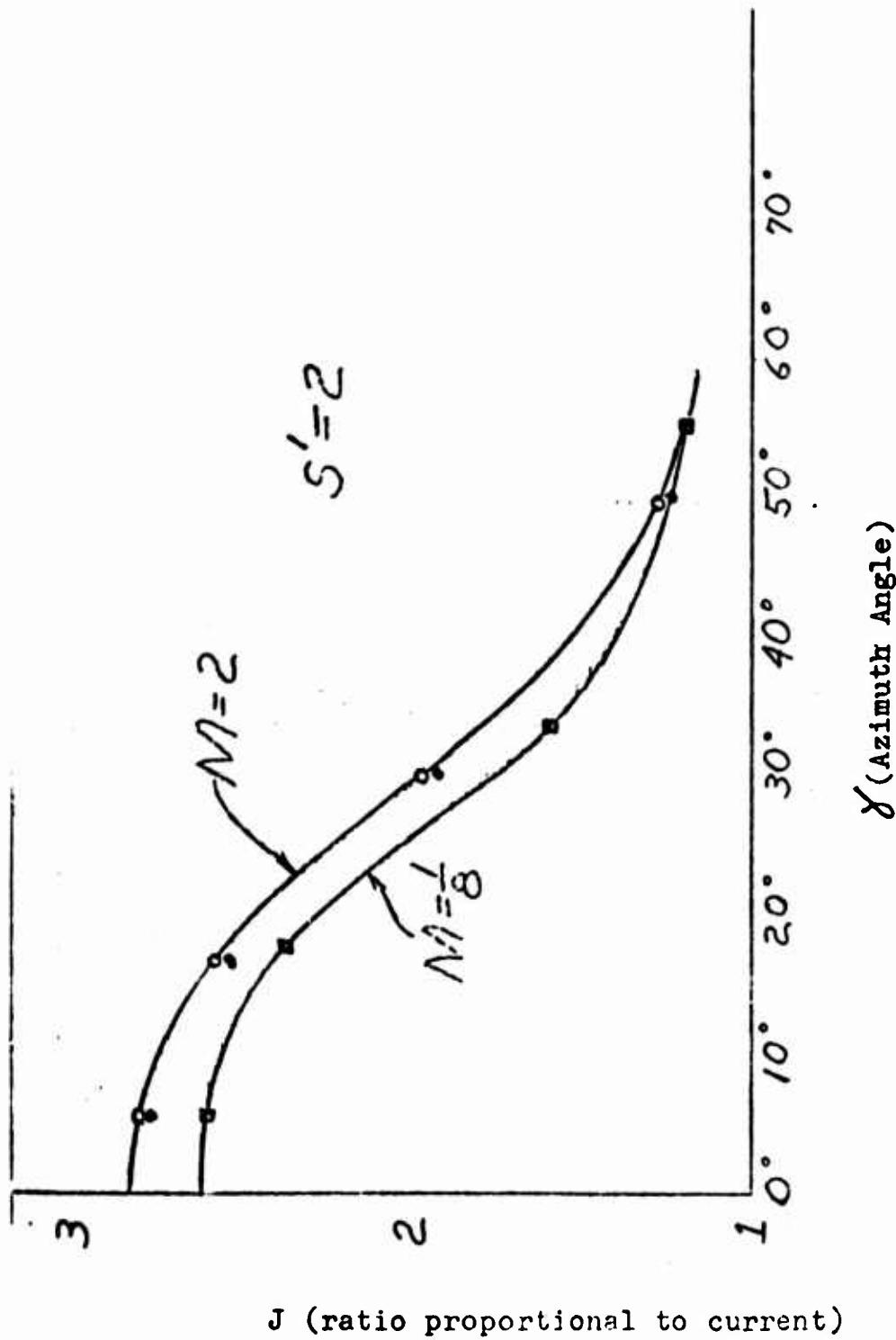
Figure 14. Current Distribution Around Cylinder for S' = 2.

30
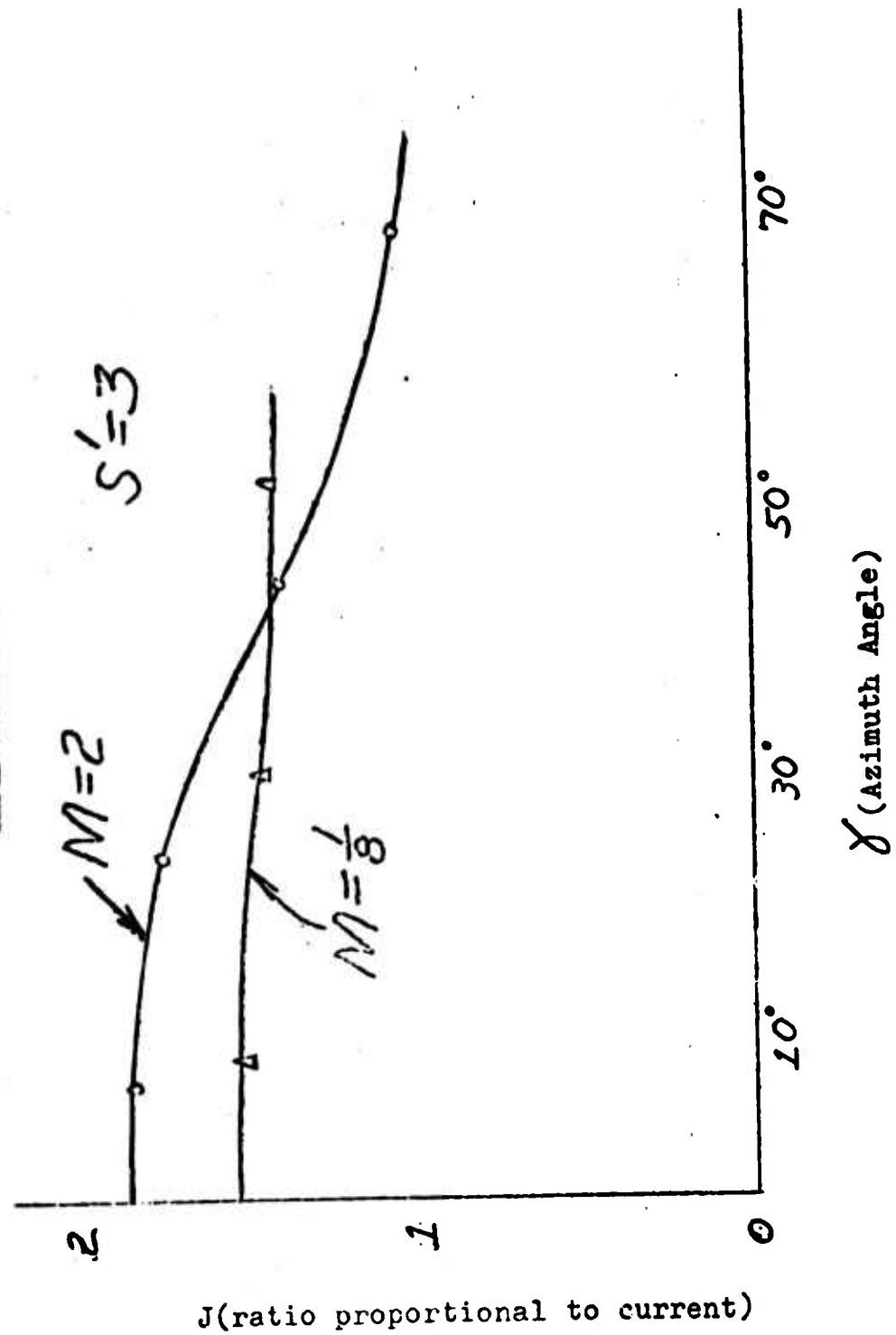
Figure 15. Current Distribution Around Cylinder for S' = 3.
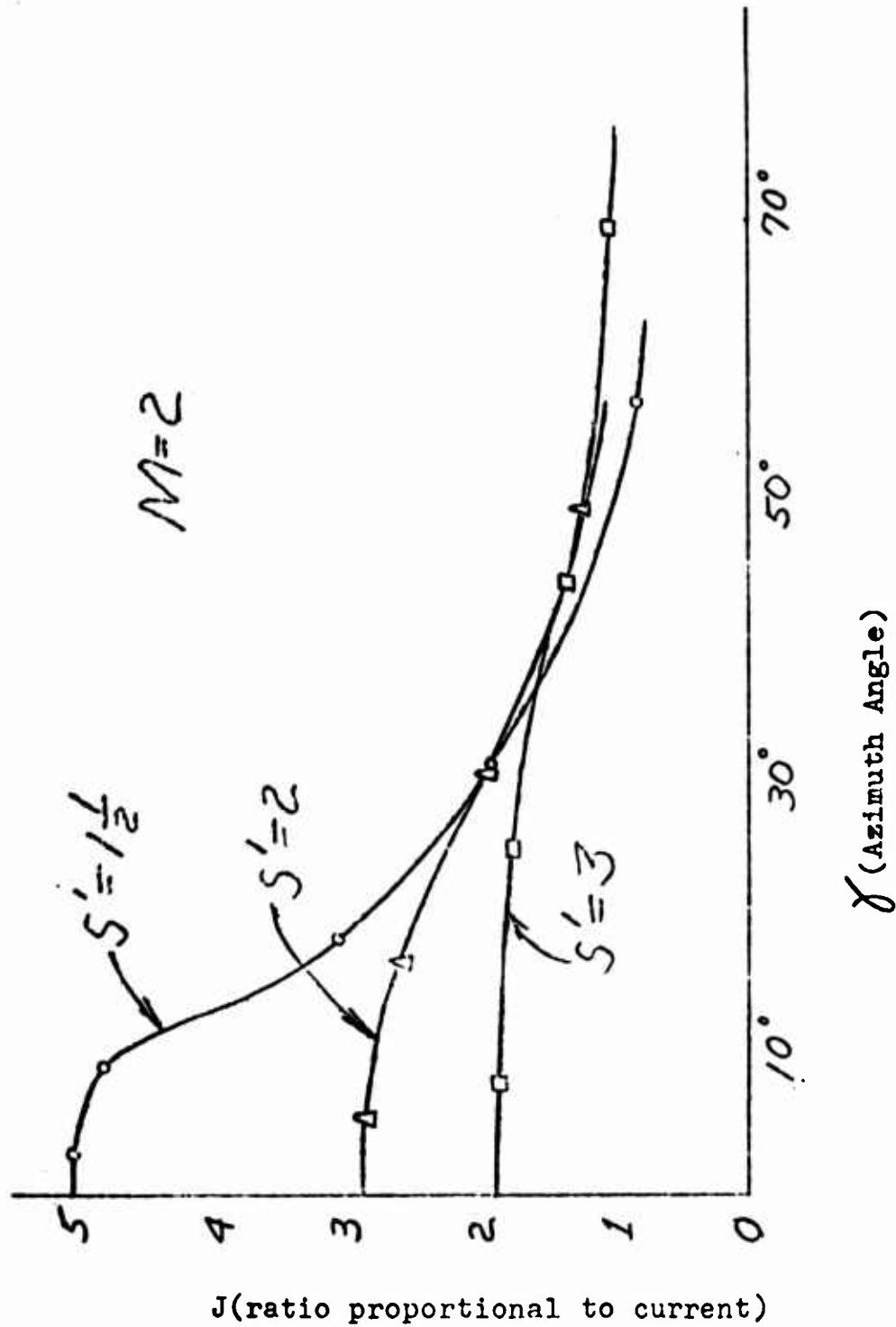
Figure 16. Current Distribution Around Cylinder for M = 2.

"error" is the boundary layer about the cylinder. As can be seen from Figures 6 and 12, the trajectories in the vicinity of the stagnation point are "turning up" abruptly near the cylinder. If the ions were "trapped" in the boundary layer prior to the time they "turned up", the low velocities in the boundary layer would again allow the electric field to dominate the ion motion and a smaller (γ) would be obtained.

For case (2), unsteady circulation and constant mobility, it was decided to consider one value of S' (2), three values of M (2, 0.5, 0.125), the maximum value of the oscillating lift coefficient (C_L), and a Strouhal number of 0.21 (which is the Strouhal number in Dr. Velkoff's work.) The maximum lift coefficient was measured by Gerrard and is about 1.5 at a Reynolds number of 10^5. This Reynolds number corresponds to the experiment. With a Strouhal of 0.21, the maximum "time" required for an ion to reach the cylinder is approximately $\frac{1}{4}$ of a cycle of the oscillating circulation. This time is so short that the circulation is virtually constant during the whole trajectory. Figures 17, 18, 19 show the trajectories for constant positive and constant negative circulation. At a fixed elapsed time the extreme values of the ion's angle with respect to the cylinder is shown by points A (positive circulation) and A' (negative circulation on Figure 17. The short time required for the ion to reach the cylinder makes the ion currents sensitive to the unsteady flow. Consequently it would be expected that the currents would be oscillating at the Strouhal frequency and that these currents should be measurable. This fact was amply demonstrated in the oscillo-scope photographs of Dr. Velkoff's experiment. For purely theoretical reasons, it was decided to plot the ion trajectories for the case when it requires one cycle ... of the oscillating circulation for the ion to traverse the gap and the case where it takes "many" cycles for a traverse. This was done by increasing the Strouhal number to unheard of dimensions. These trajectories are shown in Figures 20 and 21. An interesting result was obtained when an attempt to find the time dependent current at the stagnation point was made. The idea was to "send" a large number of ions off the corona wire at fixed time intervals which were much larger than the ion traverse time and to count the number of ions which reached an "electrode" at the cylinder in each interval. For this calculation, S' was 2, M was 0.5, C_L was 1.5, and S_T was 0.21. The cycle was broken into twelve intervals and twenty-six "stations" taken around the corona wire to an angle (α) of 30°. This maximum angle was selected by consider-ing the minimum intersection angle (γ) which was produced by the ion trajectory for the appropriate negative circulation. (γ) gave the size of the electrode (which was approximately 0.4 inches for a 6 inch diame-ter cylinder). Ions leaving at an angle greater than 30° could not intersect with this "electrode." The result of this calculation was

Time Interval	1	2	3	4	5	6	7	8	9	10	11	12
Ion Count	15	11	8	7	8	11	16	20	23	24	23	20

33
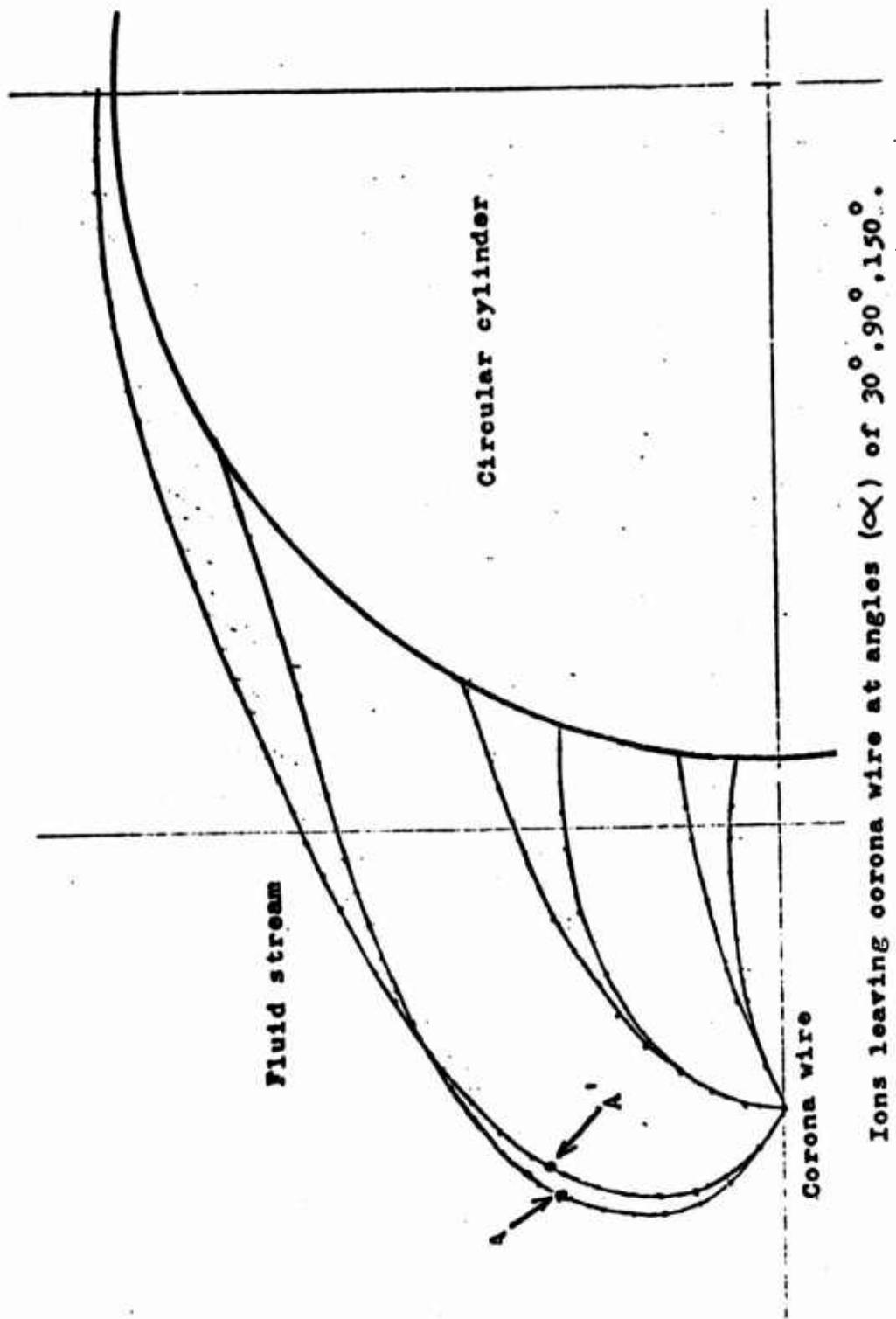
Figure 17. Ion Trajectories for $M = .5$, $S' - 1.5$, $S_T = .21$.
(Maximum dispersion of ions originating from common locations)
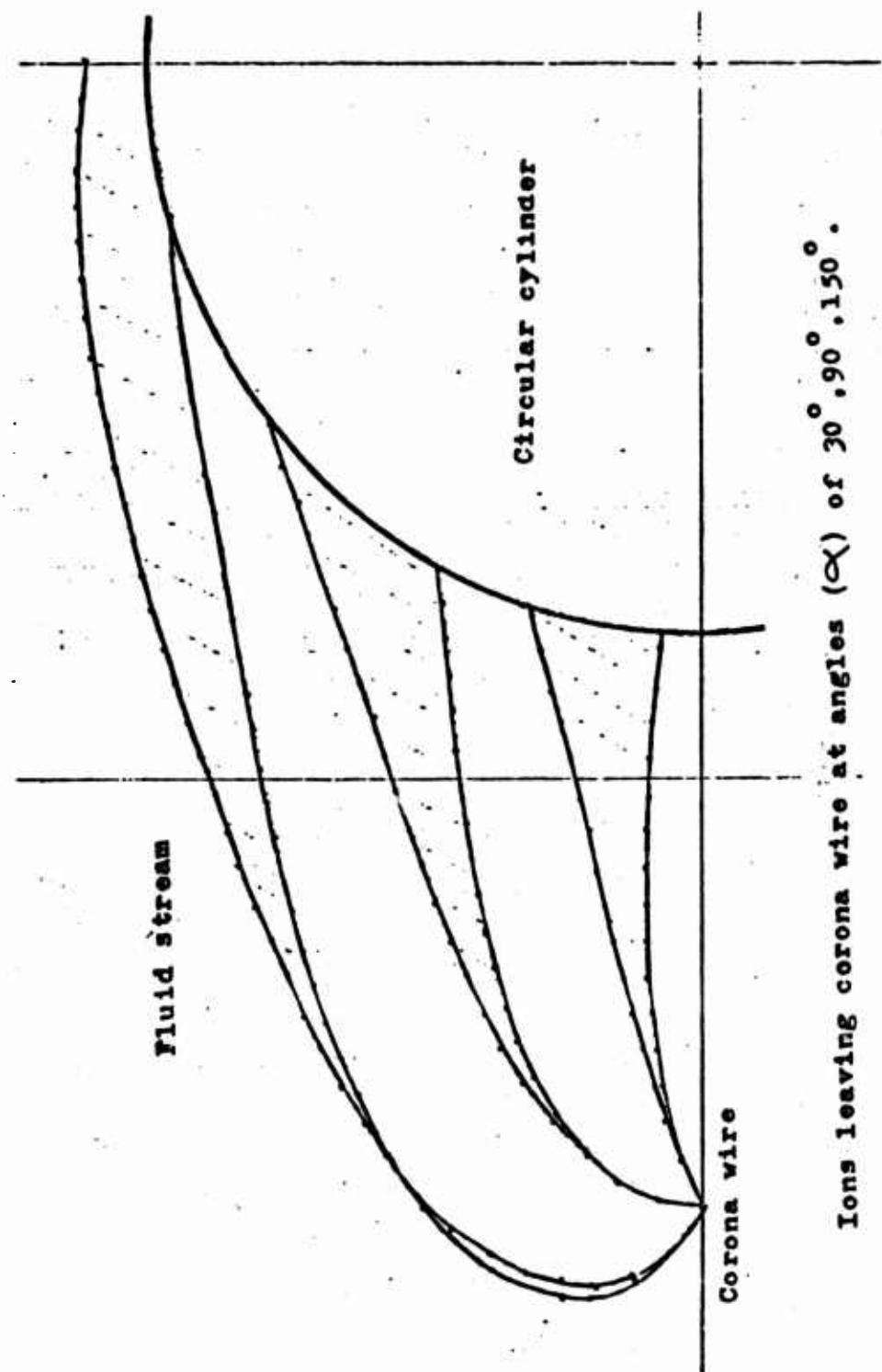
Figure 18. Ion Trajectories for M = .5, S' = 2, S_T = .21.
(Maximum dispersion of ions originating from common locations)

Ions leaving corona wire at angles (α) of $30°, 90°, 150°$.
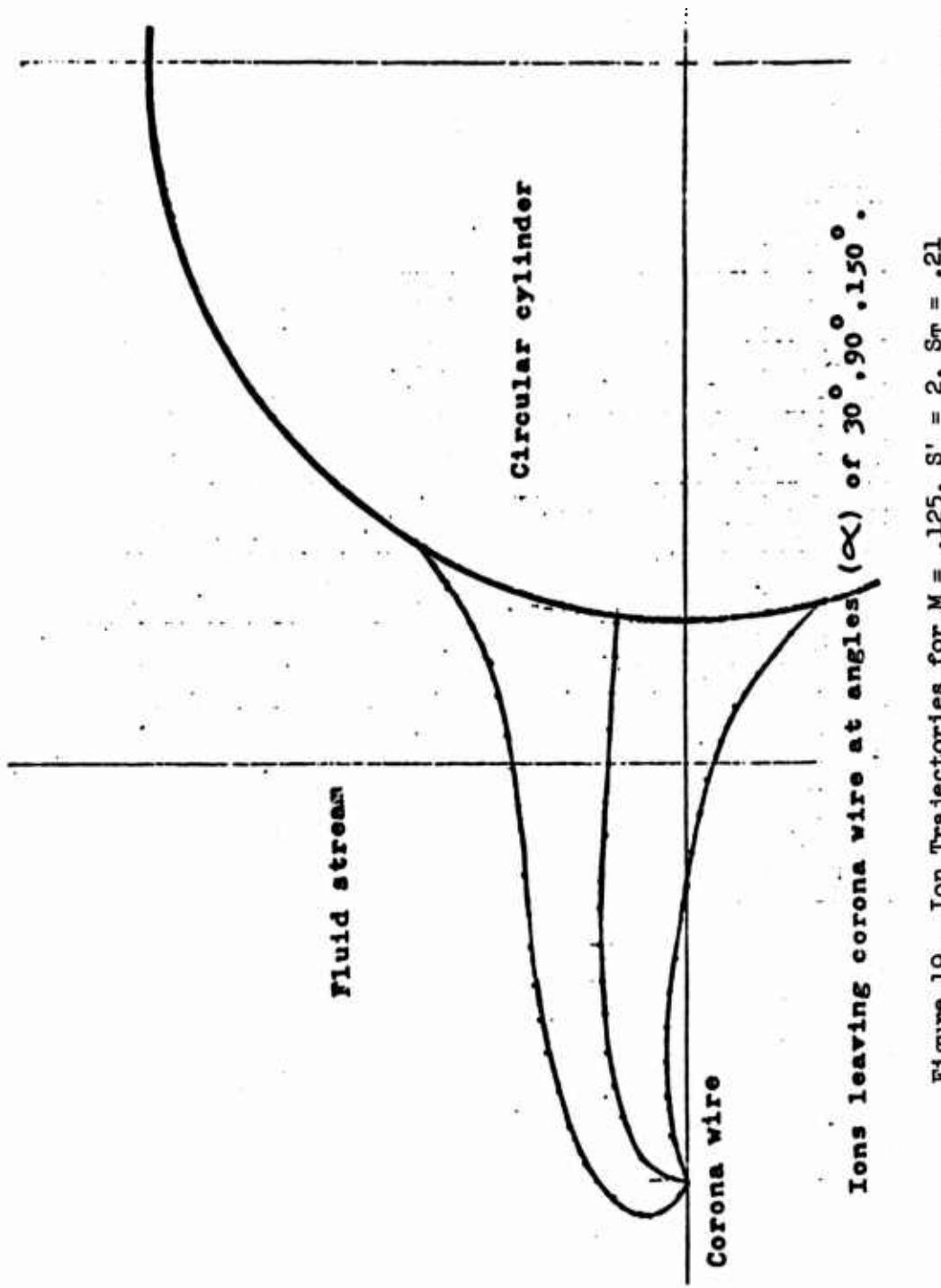
Figure 19. Ion Trajectories for M = .125, S' = 2, S_T = .21
(Maximum change in ion trajectories from negative circulation)
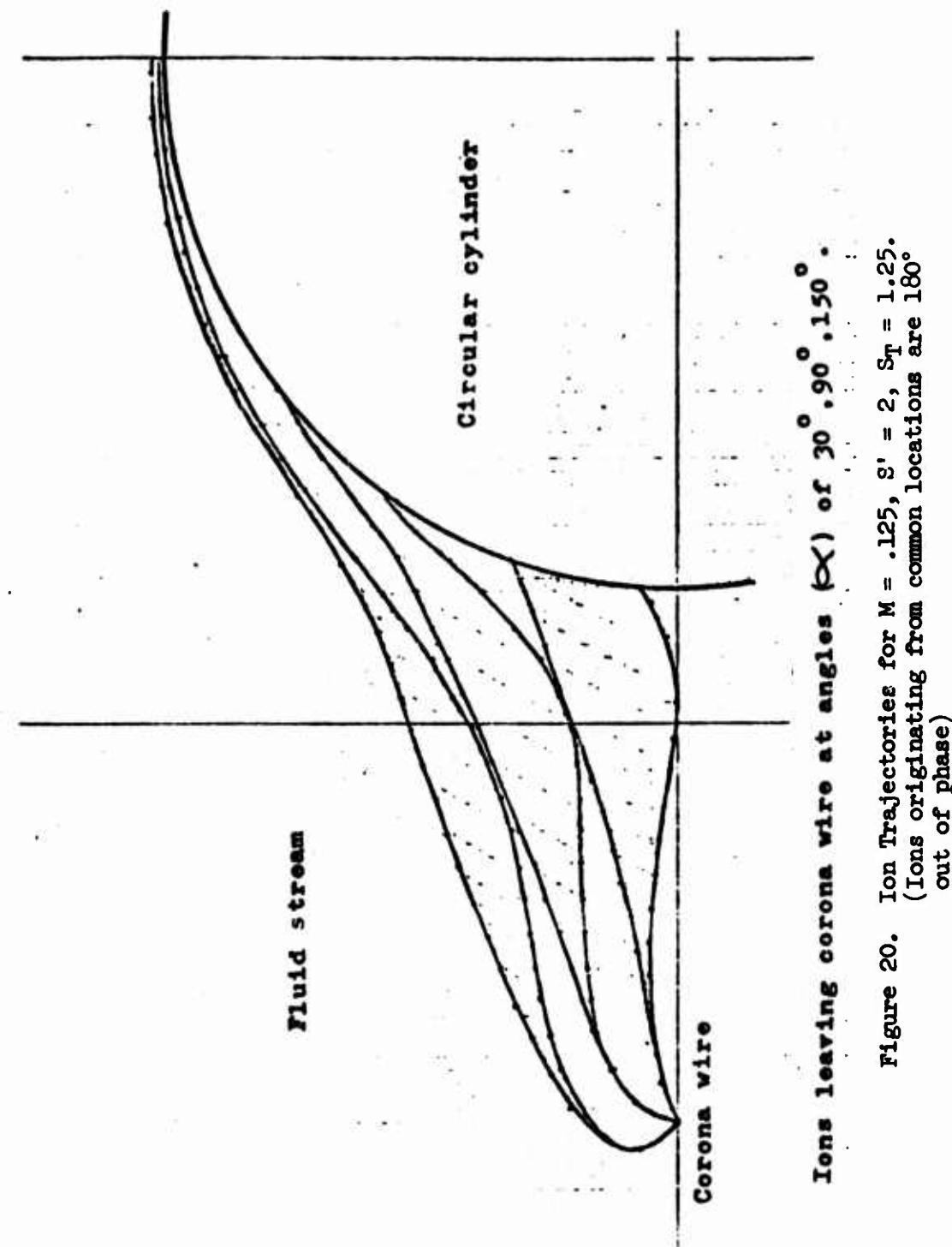
Figure 20. Ion Trajectories for M = .125, S' = 2, S_T = 1.25.
(Ions originating from common locations are 180°
out of phase)

Ions leaving corona wire at angles (α) of 30°, 90°, 150°.

37

Ions leaving corona wire at angles (α) of $30^{\circ}, 90^{\circ}, 150^{\circ}$.
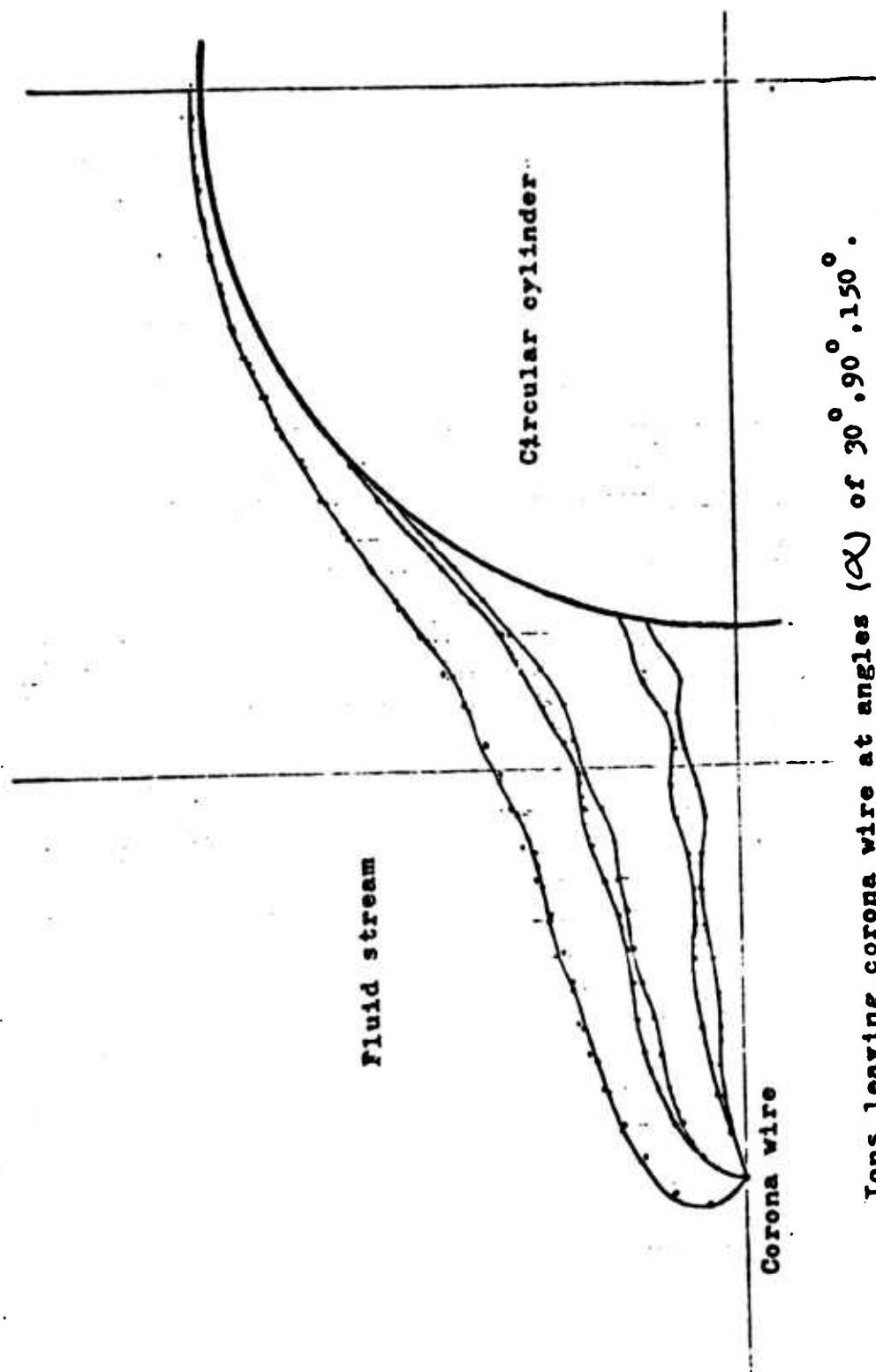
Figure 21. Ion Trajectories for M = .125, S' = 2, S_T = 5.
(Ions originating from common locations are 180°
out of phase)

38

However, the above count includes only those ions reaching the electrode from one side of the corona wire. Since the electrode chosen was symmetrical with regard to the axis, the ions leaving the "bottom" of the corona wire are 180 degrees out of phase with the "top." Consequently, to arrive at the total amount of ions reaching the electrode in each interval we must add the totals of time interval (n) with time interval (n+6) (which are 180° out of phase). If this is done all the time intervals have 31 ions each! Therefore, a constant current would be measured at the stagnation point even though the ion trajectories are time varying. Dr. Velkoff's data shows that although there is some variation in the stagnation point current, it is definitely not varying at the Strouhal frequency (as so many currents measured elsewhere are). An attempt to calculate the ion current at an angle (γ) of 54° proved inconclusive. The "sample" was decreased by one-half because of computer time limitations. Consequently the total amount of ions reaching the "electrode" was not sufficient. However the trend toward a time-varying current was seen (as the experimental data shows).

For case (3), zero circulation and variable mobility, S' was again chosen as (0.5, 0.125) and $\frac{1}{2}\frac{PU^2}{po}$ took on two values (0.09, 0.33). The value of 0.09 was chosen because it represents the maximum for air for incompressible flow around a cylinder. The larger value (0.33) was chosen because it is a mathematical maximum (approximately). If $\frac{1}{2}\frac{PU^2}{po}$ is larger than 1/3, negative absolute pressures would be obtainable from Bernoulli's equation. The results are plotted in Figures 22, 23, and 24. There is little difference between Figure 22 and Figure 12, of which the only difference is the variable mobility with $\frac{1}{2}\frac{PU^2}{po} = 0.09$. Figures 23 and 24 are interesting but are probably purely speculative, since $\frac{1}{2}\frac{PU^2}{po} = 0.33$ would lead to compressible flow for air (and probably many other fluids). From Figure 23 and 24 it would seem probable that the problem of ion trajectories in compressible flow would be interesting.

Of all the dimensionless parameters found in the trajectory analysis, probably the most far reaching one is the number $M = \frac{KV}{(\eta_2 - \eta_1)r_2 U}$. As can be seen from a comparison of Figures 4 through 12, the larger values of M are characterized by trajectories which are strongly influenced by the electric field. The lower values of M have trajectories which more nearly simulate the fluid streamlines. M can be thought of as being the ratio of $\frac{K_0 V}{(\eta_2 - \eta_1)r_2}$ to U. Therefore, qualitatively, M is the approximate ratio of the ion velocity due to the electric field to the ion velocity due to the fluid velocity field.

Circular cylinder

Fluid stream

Corona wire

Ions leaving corona wire at angles (α) of $30°$, $60°$, $90°$, $120°$, $150°$.

Figure 22. Ion Trajectories for $M = .125$, $S' = 2$, $\frac{\frac{1}{2} \rho U^2}{po} = .09$.
(Variable mobility)

40

Ions leaving corona wire at angles (α) of $30°$, $60°$, $90°$, $120°$, $150°$.
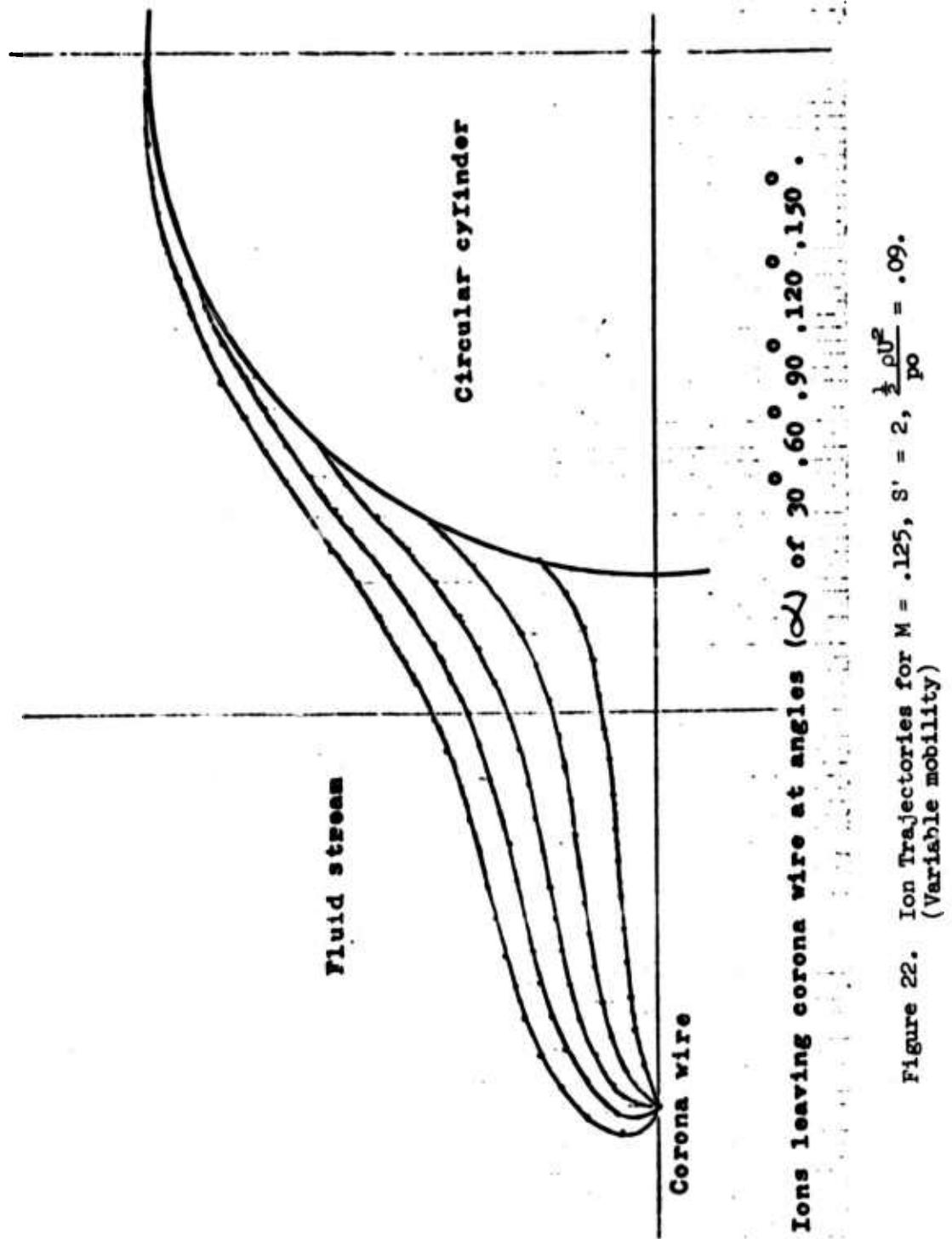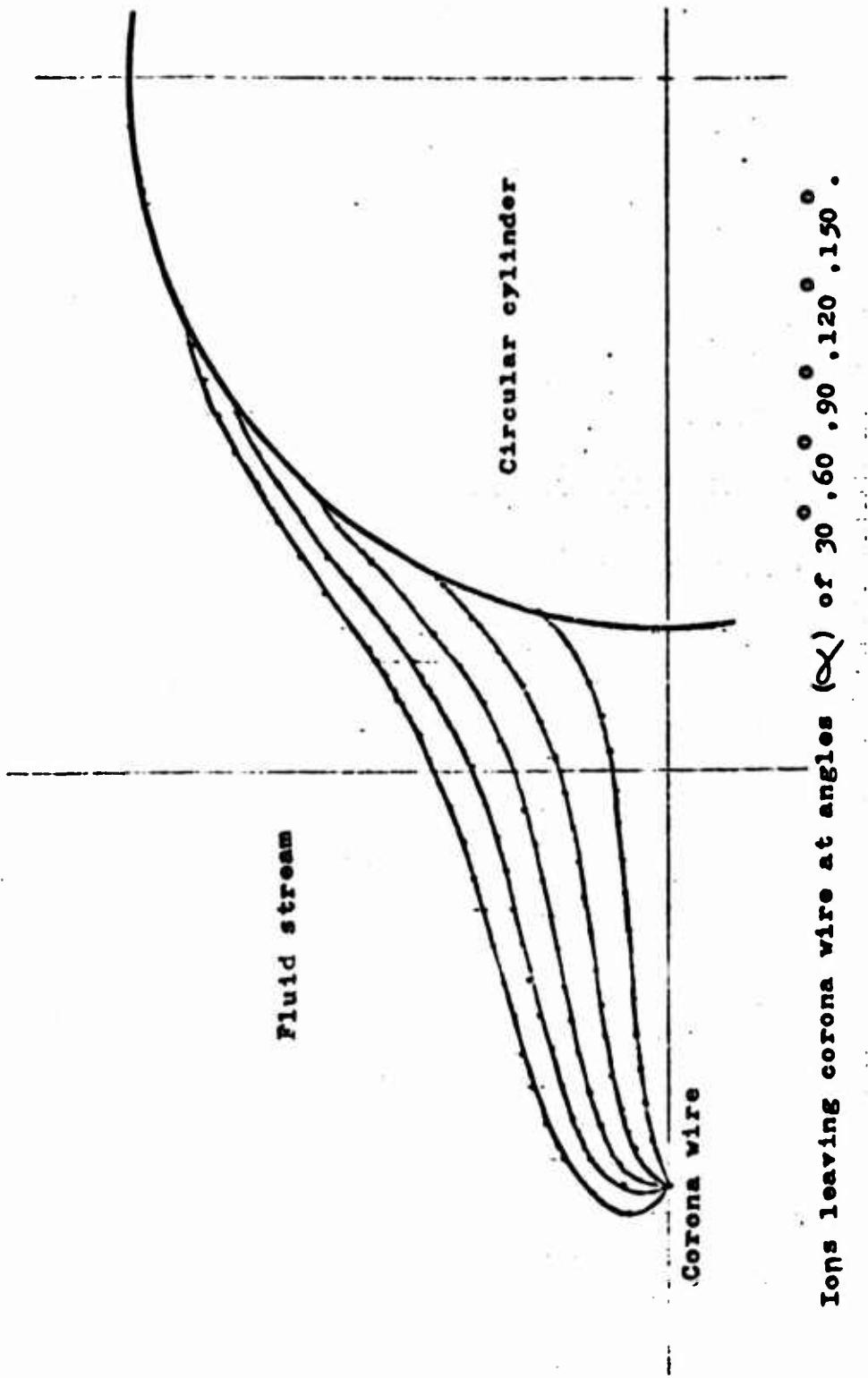
Figure 23.   Ion Trajectories for $M = .125$, $S' = 2$, $\frac{\frac{1}{2}\rho U^2}{po} = .33$
(Variable mobility)

Fluid stream

Circular cylinder

Corona wire

Ions leaving corona wire at angles (α) of $30°$, $60°$, $90°$, $120°$, $150°$.

Figure 24. Ion Trajectories for $M = .50$, $S' = 2$, $\dfrac{\frac{1}{2}\rho U^2}{p_0} = .33$. (Variable mobility)

42

V. CONCLUSIONS

Qualitatively at least, this analysis verifies the dependence of the ion currents measured at the cylinder on the vortex shedding frequency (or Strouhal number) characteristic of flow about a circular cylinder. The feature of the ion trajectories that makes this so is the short time required for an ion to traverse the corona wire - cylinder gap relative to the period of the vortex shedding. If the period of the vortex shedding was small with respect to the ion traverse time, the trajectories would vary little and consequently the ion currents would not be varying sufficiently to be measurable. Figure 21 shows this clearly; especially the longest trajectories. Fortunately Figure 21 is hypothetical.

Probably the most interesting result of this work was the "ion-count" calculation at the stagnation point. If anything, it shows possible trouble in analyzing the ion currents obtained in experiments. This calculation shows the definite periodicity of the ions reaching the stagnation point electrode and also the fact that the sum effect of the ions is non-periodic. Dr. Velkoff's experiment shows the stagnation point current to be randomly varying (and at times constant). It would be a false assumption to assume the currents measured at the stagnation point are characteristic of stagnation points. There should have been a similar periodic behavior at the stagnation point as there was at different locations in the front and rear of the cylinder. The periodic current would have been manifest at the stagnation point if the corona wire was rotated to some angle with respect to the wire - cylinder axis.

The effect of the variation in ion mobility for incompressible flow seems negligible. However, Figures 23 and 24 indicate that ion trajectories for compressible flow, i.e. larger pressure variations, would be very interesting.

For a given geometry and potential difference the free stream velocity has little effect on the average currents at the cylinder. This would indicate that oscillations of the free stream velocity would not be as measurable as the vortex shedding induced oscillations. This situation, i.e. ion currents measuring one oscillation and ignoring another oscillation of the flow in the same fluid stream, may be beneficial or harmful (it could lead to misinterpretation of the current measurements).

The average ion currents are a relatively sensitive function of the spacing of the corona wire relative to the cylinder.

These currents are even more sensitive than Figure 16 indicates since the absolute value of the electric field (and consequent ionization of the fluid) would decrease as the spacing is increased.

43

REFERENCES

1. Bateman, H., _Partial Differential Equations of Mathematical Physics_, Dover Publications, New York, 1944.

2. Cobine, J. D., _Gaseous Conductors_, Dover Publications, Inc., New York, 1958.

3. Dettman, John W., _Applied Complex Variables_, The Maxmillan Company, New York, 1965.

4. Fung, Y. C., "Fluctuating Lift and Drag Acting on a Cylinder in a Slow at Supercritical Reynolds Number," _J. Aerospace Sci._, Vol. 27, 1960, p. 801.

5. Gerrard, J. H., "An Experimental Investigation of the Oscillating Lift and Drag of a Circular Cylinder Shedding Turbulent Vortices," _J. Fluid Mechanics_, Vol. 11, 1961, p. 244.

6. Goldstein, S., _Modern Development in Fluid Mechanics_, 2 Vols., Oxford University Press, London, 1938.

7. Lawson, Maurice O., "Ion Generation by Corona Discharge for Electro-Fluid Dynamic Energy Conversion Processes," Aerospace Research Laboratories, Presented at the Sixth Agard Combustion and Propulsion Colloquium, Cannes, France, 16-20 March 1964.

8. Loeb, L. B., _Electrical Coronas, Their Basic Physical Mechanisms_, University of California Press, Berkeley, 1965.

9. Moon and Spencer, _Field Theory for Engineers_, D. Van Nostrand Company, Inc., Princeton, New Jersey, 1961.

10. Morkovin, M. V., "Flow Around Circular Cylinder--A Kaleidoscope of Challenging Fluid Phenomena," _Symposium on Fully Separated Flows_, ASME, United Engineering Center, 345 East 45th Street, New York 17, New York, 1964.

11. Panofsky and Phillips, _Classical Electricity and Magnetism_, Addison-Wesley Publishing Co., Inc., Reading, Massachusetts, 1962.

12. Roshko, A., "Experiments on the Flow Past a Circular Cylinder at Very High Reynolds Number," _J. Fluid Mechanics_, Vol. 10, 1961, p. 345.

13. Schlichting, Herman, _Boundary Layer Theory_, McGraw-Hill Book Company, New York, 1968.

14. Smythe, William R., _Static and Dynamic Electricity_, McGraw-Hill Book Company, New York, 1968.

15. Streeter, V. L., _Fluid Dynamics_, McGraw-Hill Book Company, New York, 1948.

16. Velkoff, H. R., Unpublished results of corona-ciruclar cylinder experiment.   Ohio State University.

17. Wylie, C. R., Advanced Engineering Mathematics, McGraw-Hill Book Company, New York, 1966.

APPENDIX A

FIELD THEORY, POISSON'S AND LAPLACE'S EQUATIONS,

COMPLEX POTENTIALS AND METRIC COEFFICIENTS

Preceding page blank

Consider a region of space η, each point of which is associated one or more numbers representing a physical quantity. The numbers may specify temperature, pressure, velocity, electric field strength, etc. These values, for one kind of physical quantity, constitute a physical field. Therefore, we may speak of a thermal field, a gravitational field, an electric field. The mathematical theory of the subject is called field theory. (pp. 64-70, Reference 9)

A point $\vec{P}$ in euclidean 3-space is designated by three numbers, which may be written (X_1, X_2, X_3). Suppose there is associated a scalar point function with each point in an arbitrary region η. This function may also be varying with time (t).

$$\varphi = \varphi(X_1, X_2, X_3, t) \tag{1}$$

The field is then said to be a scalar field. An example is the temperature distribution on a body.

Or suppose there is associated a vector point function with each point (and time) in the region η.

$$\vec{F} = \vec{F}(X_1, X_2, X_3, t) \tag{2}$$

The field is then said to be a vector field. An example is the electric field strength in an electric field.

The scalar field associated with a point is specified by one number. A vector field associated with some point is designated by three numbers, F_1, F_2, F_3.

$$\vec{F} = (F_1, F_2, F_3)$$

where F_1, F_2, and F_3 are magnitudes of the components of $\vec{F}$. Or unit vectors may be employed.

$$\vec{F} = \vec{a_1} F_1 + \vec{a_2} F_2 + \vec{a_3} F_3$$

For any orthogonal coordinate system, the magnitude of the vector is

$$\left| \vec{F} \right| = \left[(F_1)^2 + (F_2)^2 + (F_3)^2 \right]^{1/2}$$

Consider any vector field $\vec{F}$ (Figure 25). $\vec{P}$ is enclosed in a small

volume $\Delta\eta$ and the total flux of $\vec{F}$ through the surface of this volume (at a fixed time) is

$$\oint |\vec{F}| \cos \alpha \, dA = \oint \vec{F} \cdot \vec{dA}$$

where $\vec{dA}$ is a vector whose magnitude equals the area dA and whose direction is that of the outward-drawn normal to the surface dA. The angle α is between $\vec{F}$ and $\vec{dA}$.

A quantity called the <u>divergence</u> of $\vec{F}$ is defined by the equation,

$$\text{div } \vec{F} = \lim_{\Delta\eta\to 0} \frac{\oint \vec{F} \cdot dA}{\Delta\eta} \tag{3}$$

This is a general definition of the divergence which is applicable to any coordinate system.

Equation (3) is another way of writing the <u>Gauss' theorem</u>.

$$\int_\eta \text{div } \vec{F} \, d\eta = \oint_S \vec{F} \cdot dA \tag{4}$$

when S is the surface that encloses η.

Divergence is a measure of the strength of the <u>source</u> at $\vec{P}$.

Another quantity called the <u>curl</u> of F can be defined by the equation (again for a fixed time)

$$\text{curl } \vec{F} = \vec{a} \lim_{\Delta A \to 0} \frac{\oint_C \vec{F} \cdot dS}{\Delta A} \tag{5}$$

where the plane of C (Figure 26) is so oriented that a maximum value is obtained for the integral, and where $\vec{a}$ is a unit vector perpendicular to this plane. Equation (5) is related to Stokes' theorem which associates the surface integral of curl $\vec{F}$ and the line integral of $\vec{F}$:

$$\int_S \text{curl } \vec{F} \cdot \vec{dA} = \oint_C \vec{F} \cdot \vec{dS} \tag{6}$$

Fields may be classified in terms of the divergence and curl. If

$$\text{div } \vec{F} = 0$$
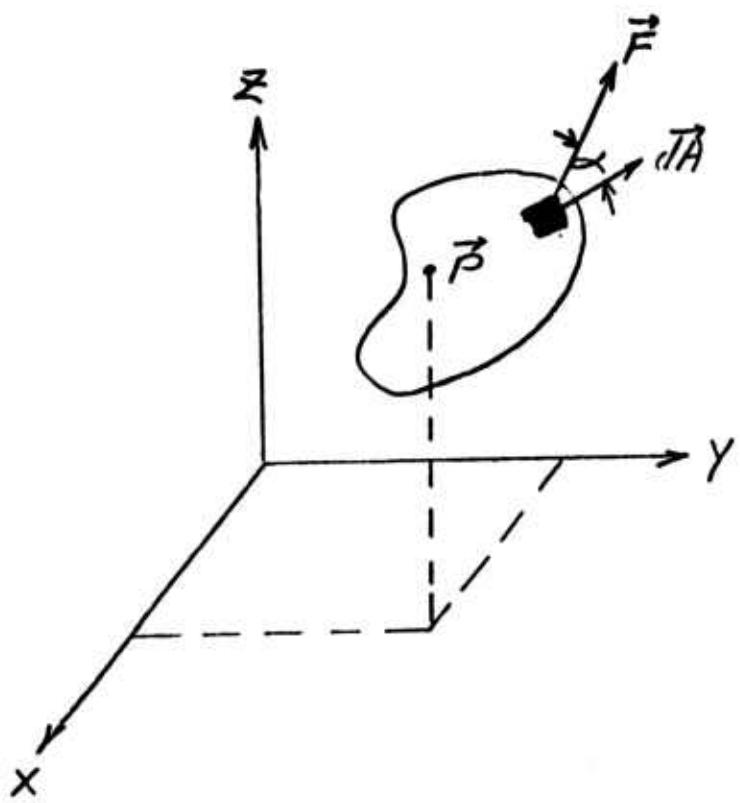
Figure 25.   Divergence

Figure 26.   Curl

51
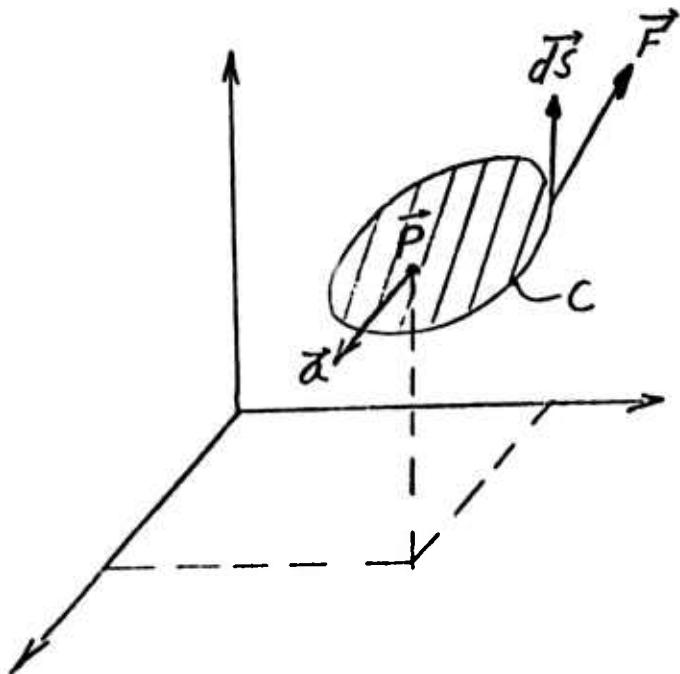
of all points in a region, the field is said to be _solenoidal_ in that region. This means there are no sources or sinks in that region--every line of flux that enters the region also leaves the region.

If, at every point in the region,

$$\text{curl } \vec{F} = 0$$

the field is said to be _irrotational_ in that region.

Consider two fixed points A and B in a vector field, Figure 27. The line integral from A to B, along a path 1:

$$\int_{(AB)_1} \vec{F} \cdot \vec{dS}$$

may be called the _potential_ φ_B at B with respect to A. Take another path 2:

$$\int_{(AB)_2} \vec{F} \cdot \vec{dS}$$

which may equally well be said to define the potential φ_B. Generally, the two integrals are not equal, so that φ_B will not be a scalar point function but will depend also on the path. If the line integral depends on the path--no scalar potential exists.
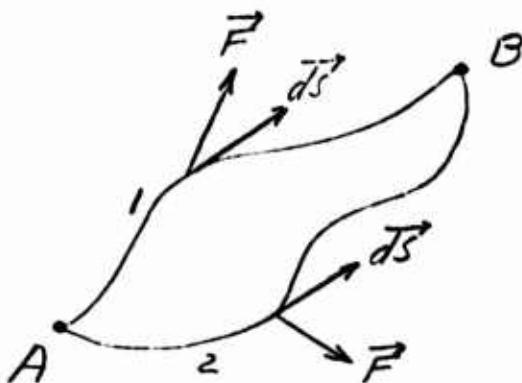
Figure 27

For the case that

$$\int_{(AB)_1} \vec{F} \cdot \vec{dS} = \int_{(AB)_2} \vec{F} \cdot \vec{dS}$$

we can write

$$\int_{(AB)_1} \vec{F} \cdot \vec{dS} - \int_{(AB)_2} \vec{F} \cdot \vec{dS} = 0$$

but

$$\int_{(AB)_2} \vec{F} \cdot \vec{dS} = -\int_{(BA)_2} \vec{F} \cdot \vec{dS}$$

Therefore

$$\int_{(AB)_1} \vec{F} \cdot \vec{dS} + \int_{(BA)_2} \vec{F} \cdot \vec{dS} = 0$$

or the line integral about a closed path through A and B is

$$\oint \vec{F} \cdot \vec{dS} = 0$$

And if this is true for any path in the field

$$\text{curl } \vec{F} = 0$$

at every point. Under these circumstances, a scalar potential φ is uniquely defined at any point B in the field. Therefore, the necessary and sufficient condition for the existence of a scalar potential φ is that

$$\text{curl } \vec{F} = 0$$

Therefore, for irrotational field at a fixed time, define

$$\varphi_B - \varphi_A = -\oint \vec{F} \cdot \vec{dS}$$

But

$$\varphi_B - \varphi_A = \oint_A^B d\varphi = -\oint_A^B \vec{F} \cdot \vec{dS}$$

$$d\varphi = \frac{\partial \varphi}{\partial x_1} dx_1 + \frac{\partial \varphi}{\partial x_2} dx_2 + \frac{\partial \varphi}{\partial x_3} dx_3$$

53

Therefore

$$\frac{\partial \varphi}{\partial x_1} \, dx_1 + \frac{\partial \varphi}{\partial x_2} \, dx_2 + \frac{\partial \varphi}{\partial x_3} \, dx_3 = - \left[F_1 dx_1 + F_2 dx_2 + F_3 dx_3 \right]$$

And, since dx_1, dx_2, and dx_3 are independent of each other,

$$F_1 = - \frac{d\varphi}{dX_1} , \quad i - 1, 2, 3$$

or

$$\vec{F} = - \text{grad } \varphi$$

For a solenoidal field

$$\text{div } F = 0$$

Therefore,

$$\text{div } \vec{F} = \text{div}(-\text{grad } \varphi) = - \text{div grad } \varphi$$

$$- \text{div grad } \varphi = - \nabla^2 \varphi = 0$$

For the special case of Cartesian coordinates

$$\nabla^2 \varphi = \frac{\partial^2 \varphi}{\partial x^2} + \frac{\partial^2 \varphi}{\partial y^2} + \frac{\partial^2 \varphi}{\partial z^2}$$

For a fluid, the flux of mass at a point (per cross-sectional area is given by $\rho \vec{V}_F$ where ρ is the density and $\vec{V}_F$ is the velocity at some point. For no sources or sinks the divergence of this quantity is zero.

$$\text{div } \rho \vec{V}_F = 0$$

For an incompressible fluid

$$\rho \text{ div } \vec{V}_F = 0$$

or

$$\text{div } \vec{V}_F = 0$$

This may be written in Cartesian coordinates as

$$\frac{\partial U}{\partial x} + \frac{\partial V}{\partial y} + \frac{\partial W}{\partial z} = 0$$

where U, V, W are the velocity components in the x, y, and z directions, respectively. This is the continuity equation for incompressible fluids.

For irrotational fluids the velocity can be expressed as the negative of the gradient of a potential

$$\vec{V}_F = - \text{ grad } \varphi_F$$

$$U = - \frac{\partial \varphi_F}{\partial \varphi}$$

$$V = - \frac{\partial \varphi_F}{\partial y}$$

The irrotational fluid criteria is satisfied for inviscid fluids. Therefore, the velocity field of an inviscid fluid can be determined from solutions of

$$\nabla^2 \varphi = 0$$

(which is called <u>Laplace's equation</u>) for the desired boundary conditions.

<u>Gauss' law for electric</u> fields is (Reference 17)

$$\oint_S \vec{D} \cdot \vec{dA} = Q$$

which asserts that the integral of the normal component of the electric flux density over any closed surface S is equal to the total electric charge enclosed by S.

By Gauss' theorem

$$Q = \int_\eta \rho_e d\eta = \oint \vec{D} \cdot \vec{dA} = \int_\eta \text{ div } \vec{D} \, d\eta$$

so

$$\text{div } \vec{D} = \rho_e$$

or the divergence of $\vec{D}$ at any point P is equal to the charge desnity at that point. For free space

$$\rho_e = 0$$

and therefore

$$\text{div } \vec{D} = 0$$

For an isotropic and homogeneous medium

55

$$\vec{E} = \frac{\vec{D}}{\epsilon}$$

where E is the electric field strength and ϵ is the capacitivity (or permittivity).

Faraday's law for electromagnetic fields is (Reference 17)

$$\int_C \vec{E} \cdot \vec{dS} = - \frac{\partial}{\partial t} \oint \vec{B} \cdot dA$$

which asserts that the integral of the tangential component of the electric field strength vector around any closed curve C is equal but opposite in sign to the rate of change of the magnetic flux passing through any surface spanning C. If $\vec{B}$ (magnetic flux density) is zero

$$\int_C \vec{E} \cdot \vec{dS} = 0$$

and

$$\text{curl } \vec{E} = 0$$

and the electric field is irrotational and $\vec{E}$ can be expressed as the gradient of some potential function φ_E

$$\text{div } \vec{D} = \text{div } \epsilon \vec{E} = \rho_e$$

$$\text{div } \llcorner = \frac{\rho_e}{\epsilon} = \text{div}(-\text{grad } \varphi_E)$$

$$\nabla^2 \varphi_E = - \frac{\rho_e}{\epsilon}$$

This equation is known as Poisson's equation and for $\rho_e = 0$

$$\nabla^2 \varphi_E = 0$$

which again is Laplace's equation.

Laplace's equation can be solved in a number of ways, i.e., mathematical, graphical, and experimental. The mathematical techniques are (1) separation of variables, (2) functions of a complex variable, (3) Laplace transform, and (4) numerical approximation ("relaxation" method). For this thesis complex variable technique is the predominant way in which this equation is solved.

An infinite number of solutions to the two-dimensional Laplace equation are easily obtainable from functions of a complex variable.

56

Due to the application of complex variable theory, the study of inviscid fluid flow has been greatly expanded.

When x and y in the complex number $z = x + iy$ (z has been redefined) are considered variables, then z is said to be a complex variable. Defining W as another complex variable such that (W has also been redefined) (pp. 74-77, Reference 15).

$$W = f(z) = f(x + iy)$$

W may be separated into its real part and its imaginary part, called φ and ψ, respectively

$$W = \varphi(x,y) + i\psi(x,y)$$

where φ and ψ are both real functions of x,y.

The function $f(z)$ is said to be a function of a complex variable if (1) within some region there is one and only value of $f(z)$ for each value of z and that value is finite and (2) the function has a one-valued derivative at each point within the region. Within this region the function is said to be holomorphic, regular, and analytic.

Further consideration of (2) yields relationships that must be fulfilled by a function if it is analytic. A complex derivative

$$\frac{df}{dz} = \lim_{\delta z \to 0} \frac{f(z + \delta z) - f(z)}{\delta z}$$

may approach its limit in an infinite number of ways. The different paths by which the limit may be approached are considered. For the first path, δz is allowed to approach zero in the x-direction; i.e., let $\delta y = 0$ first, then take the limit as δx approaches zero. This gives

$$\lim_{\substack{\delta y \to 0 \\ \delta x \to 0}} \frac{f(z + \delta z) - f(z)}{\delta x} = \lim_{\delta x \to 0} \frac{f(z + \delta x) - f(z)}{\delta x} = \frac{\partial f}{\partial x}$$

where the last term comes from the second term which is the definition of a partial derivative. For the second path, δz is allowed to approach zero in the y-direction by letting $\delta x = 0$ first; thus

$$\lim_{\substack{\delta x \to 0 \\ \delta y \to 0}} \frac{f(z + \delta z) - f(z)}{\delta x + i \, \delta y} = \frac{1}{i} \lim_{\delta y \to 0} \frac{f(z + \delta y) - f(z)}{\delta y} = \frac{1}{i} \frac{\partial f}{\partial y}$$

57

Since the derivative must be the same in either case if f(z) is a
function of a complex variable

$$\frac{\partial f}{\partial x} = \frac{1}{i} \frac{\partial f}{\partial y}$$

However,

$$f(z) = W = \varphi + i\psi$$

and therefore,

$$\frac{\partial f}{\partial x} = \frac{\partial \varphi}{\partial x} + i \frac{\partial \psi}{\partial x} \quad , \quad \frac{\partial f}{\partial y} = \frac{\partial \varphi}{\partial y} + i \frac{\partial \psi}{\partial y}$$

Substitution yields

$$\frac{\partial \varphi}{\partial x} + i \frac{\partial \psi}{\partial x} = \frac{1}{i} \left(\frac{\partial \varphi}{\partial y} + i \frac{\partial \psi}{\partial y} \right)$$

Equating the real parts and imaginary parts in each side of the equation
yields

$$\frac{\partial \varphi}{\partial x} = \frac{\partial \psi}{\partial y} \quad , \quad \frac{\partial \varphi}{\partial y} = - \frac{\partial \psi}{\partial x} \tag{7}$$

These relations are called the Cauchy-Riemann equations. They are not
only necessary but sufficient conditions for the function W(z) to be
called analytic.

Differentiating the first of Equations (7) with respect to x and
the second with respect to y and adding give

$$\frac{\partial^2 \varphi}{\partial x^2} + \frac{\partial^2 \varphi}{\partial y^2} = 0$$

which is the Laplace equation in two-dimensional cartesian coordinates.
Therefore, by considering φ to be a velocity potential or an electric
potential, the real part of any function of a complex variable is a pos-
sible flow field or electric field.

Similarly, differentiating the first of Equations (7) with respect
to y and the second with respect to x and subtracting one from the other

$$\frac{\partial^2 \psi}{\partial x^2} + \frac{\partial^2 \psi}{\partial y^2} = 0$$

showing that the pure imaginary part of any function of a complex variable may also be the velocity or electric potential for a field. Usually φ is considered the potential function, the ψ is called the stream function.

The functions φ, ψ are called conjugate functions; i.e., the real part of an analytic function is said to be the conjugate of the imaginary part. The curves obtained by

$$\varphi(x,y) = \text{constant}$$
$$\psi(x,y) = \text{constant}$$

form an orthogonal system in the xy-plane.

In the solution of Laplace's equation by separation of variables, the first step is to transform from Cartesian coordinates to a coordinate system that fits the boundary conditions. The work is expedited by having a general method that allows transformations to any coordinate system. Such a method is based on metric coefficients (Reference 9).

A differential length is expressed in general orthogonal coordinates (X_1, X_2, x_3) as

$$(dS)^2 = g_{11}(dx_1)^2 + g_{22}(dx_2)^2 + g_{33}(dx_3)^2$$

where the metric coefficients are

$$g_{11} = \left(\frac{\partial x}{\partial x_1}\right)^2 + \left(\frac{\partial y}{\partial x_1}\right)^2 + \left(\frac{\partial z}{\partial x_1}\right)^2$$

where x, y, and z are Cartesian coordinates.

The expressions in orthogonal coordinates for the gradient, divergence and Laplaces' equation are

$$\text{grad } \varphi = \frac{\vec{a_1}}{(g_{11})^{1/2}} \frac{\partial \varphi}{\partial x_1} + \frac{\vec{a_2}}{(g_{22})^{1/2}} \frac{\partial \varphi}{\partial x_2} + \frac{\vec{a_3}}{(g_{33})^{1/2}} \frac{\partial \varphi}{\partial x_3}$$

$$\text{div } \vec{F} = g^{-1/2}\left\{ \frac{\partial}{\partial x_1}\left[\frac{g^{1/2}}{g_{11}} F_1 \right] + \frac{\partial}{\partial x_2}\left[\frac{g^{1/2}}{g_{22}} F_2 \right] + \frac{\partial}{\partial x_3}\left[\frac{g^{1/2}}{g_{33}} F_3 \right] \right\}$$

$$\nabla^2 \varphi = g^{-1/2}\left\{ \frac{\partial}{\partial x_1}\left[\frac{g^{1/2}}{g_{11}} \frac{\partial \varphi}{\partial x_1} \right] + \frac{\partial}{\partial x_2}\left[\frac{g^{1/2}}{g_{22}} \frac{\partial \varphi}{\partial x_2} \right] + \frac{\partial}{\partial x_3}\left[\frac{g^{1/2}}{g_{33}} \frac{\partial \varphi}{\partial x_3} \right] \right\}$$

where $g = g_{11}g_{22}g_{33}$

59

APPENDIX B

ELECTRIC FIELD ANALYSIS FOR TWO PARALLEL CYLINDERS

OF DIFFERENT RADII

Preceding page blank

The electrical field around a line charge with a linear charge density q is found by means of Gauss' law for electric fields (Gauss' electric flux theorem), the surface of integration being that of a circular cylinder of radius r and unit length coaxial with the line charge. If the charge is located at the origin of coordinates in the xy-plane, this field is given by (Reference 14)

$$\vec{E} = \frac{q}{\epsilon} \frac{\vec{r}}{r^2}$$

The corresponding potential may be secured by substituting this field into

$$\vec{E} = - \text{ grad } \varphi$$

and integrating, grad φ in polar coordinates with φ a function of r only is

$$\text{grad } \varphi = \frac{d\varphi}{dr} \frac{\vec{r}}{r^2}$$

Therefore

$$\frac{q}{\epsilon} \frac{\vec{r}}{r^2} = - \frac{d\varphi}{dr} \frac{\vec{r}}{r}$$

and

$$\varphi = - \frac{q}{r} (\ln r - \ln r_o) \tag{8}$$

The complex potential function corresponding to a line charge located at an arbitrary point Zo may be derived by means of the Cauchy-Riemann equations, but it is easily written merely by inspection of Equation (8). In polar coordinates

$$Z = re^{i\theta}$$

And

$$\ln Z = \ln r + i\theta$$

Clearly from Equation (8), φ is the real part of $- q/\epsilon \ln Z$, so

$$W = \varphi + i\psi = - \frac{q}{\epsilon} \ln Z$$

is the desired complex function for a line charge at the origin. It follows that a line charge at Zo has the complex potential. (Ref. 11).

$$W = - \frac{q}{\epsilon} \ln (Z-Zo)$$

Preceding page blank

The function for n line charges situated at Z_1, Z_2, $\cdots$, Z_n is therefore

$$W = - \frac{1}{\epsilon} \sum_{S=1}^{n} q_S \, \ell n \, (Z-Z_S) \tag{9}$$

Let us superimpose the fields due to charges $+\epsilon$ at $x = a$ and $-\epsilon$ at $x = -a$.

This choice of the charge q simplifies the coefficients. From Equation (9) the expression for the complex potential becomes

$$W = - \ell n(Z-a) + \ell n \, (Z+a)$$

So

$$W = \ell n \, \frac{(Z+a)}{(Z-a)}$$

Therefore

$$W = \ell n \left(\frac{x + a + iy}{x - a + iy} \right)$$

The denominator of the natural logarithm's argument may be cleared of the complex number by multiplying the numerator and denominator by the conjugate of the denominator, hence

$$W = \ell n \, \frac{(x + a + iy)}{(x - a + iy)} \cdot \frac{(x - a - iy)}{(x - a - iy)}$$

Multiplying,

$$W = \ell n \left[\frac{x^2 - a^2 + y^2 + i(-2ay)}{(x-a)^2 + y^2} \right]$$

It can be shown that

$$\ell n(u + iv) = \ell n(u^2 + v^2) + i \, \tan^{-1} \frac{v}{u}$$

Therefore

$$W = \ell n \, \frac{\sqrt{(x^2 + y^2 - a^2)^2 + (2ay)^2}}{(x-a)^2 + y^2} + i \, \tan^{-1} \frac{-2ay}{x^2 - a^2 + y^2}$$

Now, since

$$W = \varphi + i\psi$$

64

$$\varphi = \ell n \, \frac{\sqrt{(x^2 + y^2 - a^2)^2 + (2ay)^2}}{(x-a)^2 + y^2}$$

and

$$\psi = \tan^{-1} \frac{-2ay}{x^2 - a^2 + y^2}$$

So

$$\tan \psi = - \frac{2ay}{x^2 - a^2 + y^2}$$

Multiplying both sides of the equation by the denominator of the right side gives

$$(x^2 + y^2 - a^2)\tan \psi = -2ay$$

Dividing both sides of the equation by tan ψ and adding the negative of the right side to both sides yields

$$x^2 + y^2 + \frac{2ay}{\tan \psi} - a^2 = 0$$

or

$$x^2 + y^2 + \frac{2ay}{\tan \psi} = a^2$$

Completing the square and adding to both sides

$$x^2 + y^2 + \frac{2a}{\tan \psi} \, y + \left(\frac{a}{\tan \psi} \right)^2 = a^2 + \left(\frac{a}{\tan \psi} \right)^2$$

Therefore

$$x^2 + \left(y + \frac{a}{\tan \psi} \right)^2 = a^2 \left(1 + \frac{1}{\tan \psi^2} \right)$$

But

$$\cot \psi = \frac{1}{\tan \psi}$$

$$1 + \cot^2 \psi = \csc^2 \psi$$

So

$$x^2 + (y + a \cot \psi)^2 = a^2 \csc^2 \psi$$

65

This equation is a family of circles all passing through the points (a,o) and (-a,o) with radii of

$$r_\psi = \left| \frac{a}{\sin \psi} \right|$$

and with centers at

$$y = -a \cot \psi$$

Therefore the lines of constant ψ (electrical streamlines or lines of force) are nonconcentric circles passing through what are called the poles at $x = \mp a$, $y = 0$.

It also can be shown that the lines of constant φ are also non-concentric circles. The radii of the equipotential circles are given by

$$r_\varphi = \left| \frac{a}{\sinh \varphi} \right|$$

The centers are at

$$X = a \coth \varphi$$

The lines of constant ψ and constant φ form an orthogonal net. Hence, a transformation which would be useful for solving multi-cylinder problems would be one based on the transformation.

$$W = \ell n \frac{(z + a)}{(z - a)}$$

If we substitute a coordinate (called η) for φ and another coordinate (called θ_B) for ψ, we will have a transformation which will produce a solution to Laplace's equation so that the potential φ is only a function of η. To demonstrate this (using metric coefficients) it is first necessary to find x and y as functions of η and θ_B.

So let

$$\eta + i\theta_B = \ell n \frac{(z + a)}{(z - a)}$$

Luckily,

$$\ell n \frac{1 + u}{1 - u} = 2 \tanh^{-1} u$$

Therefore,

$$\eta + i\theta_B = 2 \tanh^{-1} \frac{a}{z} = 2 \coth^{-1} \frac{z}{a}$$

66

Solving for z,

$$z = x + iy = a \coth\left(\frac{\eta + i\theta_B}{2}\right) = a \, \frac{\cosh\left(\dfrac{\eta + i\theta_B}{2}\right)}{\sinh\left(\dfrac{\eta + i\theta_B}{2}\right)}$$

But

$$\cosh(u + iv) = \cosh u \cos v + i \sinh u \sin v$$
$$\sinh(u + iv) = \sinh u \cos v + i \cosh u \sin v$$

Hence, substituting

$$x + iy = a \, \frac{\cosh \frac{\eta}{2} \cos \frac{\theta_B}{2} + i \sinh \frac{\eta}{2} \sin \frac{\theta_B}{2}}{\sinh \frac{\eta}{2} \cos \frac{\theta_B}{2} + i \cosh \frac{\eta}{2} \sin \frac{\theta_B}{2}}$$

The denominator can be cleared of the complex number as before,

$$x + iy = a \, \frac{\cosh \frac{\eta}{2} \cos \frac{\theta_B}{2} + i \sinh \frac{\eta}{2} \sin \frac{\theta_B}{2}}{\sinh \frac{\eta}{2} \cos \frac{\theta_B}{2} + i \cosh \frac{\eta}{2} \sin \frac{\theta_B}{2}} \times \frac{\sinh \frac{\eta}{2} \cos \frac{\theta_B}{2} - i \cosh \frac{\eta}{2} \sin \frac{\theta_B}{2}}{\sinh \frac{\eta}{2} \cos \frac{\theta_B}{2} - i \cosh \frac{\eta}{2} \sin \frac{\theta_B}{2}}$$

Multiplying,

$$x + iy = a \left[\frac{\cosh \frac{\eta}{2} \sinh \frac{\eta}{2} \cos^2 \frac{\theta_B}{2} + \cosh \frac{\eta}{2} \sinh \frac{\eta}{2} \sin^2 \frac{\theta_B}{2}}{\sinh^2 \frac{\eta}{2} \cos^2 \frac{\theta_B}{2} + \cosh^2 \frac{\eta}{2} \sin^2 \frac{\theta_B}{2}} + \right.$$

$$\left. \frac{i\left(\sinh^2 \frac{\eta}{2} \sin \frac{\theta_B}{2} \cos \frac{\theta_B}{2} - \cosh^2 \frac{\eta}{2} \sin \frac{\theta_B}{2} \cos \frac{\theta_B}{2}\right)}{\sinh^2 \frac{\eta}{2} \cos^2 \frac{\theta_B}{2} + \cosh^2 \frac{\eta}{2} \sin^2 \frac{\theta_B}{2}} \right]$$

Substituting the relationships

$$\cos^2 u + \sin^2 u = 1$$

$$\cosh^2 u - \sinh^2 u = 1$$

yields

$$x = iy = a \, \frac{\cosh \frac{\eta}{2} \sinh \frac{\eta}{2} - i \sin \frac{\theta_B}{2} \cos \frac{\theta_B}{2}}{\cosh^2 \frac{\eta}{2} - \cos^2 \frac{\theta_B}{2}}$$

67

Substituting the relationships

$$\cosh u \sinh u = \tfrac{1}{2} \sinh 2u$$

$$\cosh^2 u = \tfrac{1}{2}(1 + \cosh 2u)$$

$$\cos u \sin u = \tfrac{1}{2} \sin 2a$$

$$\cos^2 u = \tfrac{1}{2}(1 + \cos 2u)$$

gives

$$x + iy = a \, \frac{\tfrac{1}{2} \sinh \eta - i \, \tfrac{1}{2} \sin \theta_B}{\tfrac{1}{2}(1 + \cosh \eta) - \tfrac{1}{2}(1 + \cos \theta_B)}$$

which factors to

$$x + iy = a \, \frac{\sinh \eta - i \sin \theta_B}{\cosh \eta - \cos \theta_B}$$

Equating real and imaginary parts on both sides of the equation gives

$$x = a \, \frac{\sinh \eta}{\cosh \eta - \cos \theta_B}$$

and

$$y = -a \, \frac{\sin \theta_B}{\cosh \eta - \cos \theta_B}$$

The minus sign can be dropped since $\sin(-u) = -\sin(u)$ and $\cos(-u) = \cos(u)$ and we can let $\theta_B' = -\theta_B$ and then redefine θ_B. Therefore

$$x = a \, \frac{\sin \eta}{\cosh \eta - \cos \theta_B}$$

and

$$y = a \, \frac{\sin \theta_B}{\cosh \eta - \cos \theta_B}$$

are the desired transformation functions. This transformation is called the <u>bicylindrical</u> transformation. The name implies the use of this transformation for solving two-cylinder problems. The inverse transformation functions are

$$\eta = \ell n \, \frac{\sqrt{(x^2 + y^2 - a^2)^2 + (2ay)^2}}{(x-a)^2 + y^2}$$

68

and

$$\theta_B = -\tan^{-1} \frac{-2ay}{x^2 + y^2 - a^2}$$

For bicylindrical coordinates, it is convenient to let η range from $-\infty$ to $+\infty$, which can be done by assigning positive values of η to cylinders for which x is positive, and negative values of cylinders for which x is negative. The parameter θ_B represents the angle between lines drawn from the poles to a given point. Evidently $\theta_B = \pi$ represents a line along the x axis between x = -a and x = a; while $\theta_B = 0$ represents the remainder of the x axis. The portions of the cylinders (θ_B = constant) above the x axis are designated by positive values of θ_B, while those below the x axis are designated by negative values of θ_B. The metric coefficients for bicylindrical coordinates are obtained from (Appendix A)

$$g_{ii} = \left(\frac{\partial x}{\partial x_i}\right)^2 + \left(\frac{\partial y}{\partial x_i}\right)^2$$

Let

$$\eta = x_1 \quad , \quad \theta_B = x_2$$

So

$$g_\eta = \left(\frac{\partial x}{\partial \eta}\right)^2 + \left(\frac{\partial y}{\partial \eta}\right)^2$$

and

$$g_{\theta_B} = \left(\frac{\partial x}{\partial \theta_B}\right)^2 + \left(\frac{\partial y}{\partial \theta_B}\right)^2$$

Differentiating,

$$\frac{\partial x}{\partial \eta} = a \frac{(\cosh \eta - \cos \theta_B)\cosh \eta - \sinh \eta \sinh \eta}{(\cosh \eta - \cos \theta_B)^2}$$

$$\frac{\partial y}{\partial \eta} = -a \frac{\sin \theta_B \sinh \eta}{(\cosh \eta - \cos \theta_B)^2}$$

$$\frac{\partial x}{\partial \theta_B} = -a \frac{\sinh \eta \sin \theta_B}{(\cosh \eta - \cos \theta_B)^2}$$

$$\frac{\partial y}{\partial \theta_B} = a \frac{(\cosh \eta - \cos \theta_B)\cos \theta_B - \sin \theta_B \sin \theta_B}{(\cosh \eta - \cos \theta_B)^2}$$

69

Simplifying,

$$\frac{\partial x}{\partial \eta} = a \frac{1 - \cos \theta_B \cosh \eta}{(\cosh \eta - \cos \theta_B)^2}$$

$$\frac{\partial y}{\partial \theta_B} = a \frac{\cosh \eta \cos \theta_B - 1}{(\cosh \eta - \cos \theta_B)^2} = -\frac{\partial x}{\partial \eta}$$

Therefore

$$\left(\frac{\partial y}{\partial \theta_B}\right)^2 = \left(\frac{\partial x}{\partial \eta}\right)^2$$

Also

$$\frac{\partial y}{\partial \eta} = -\frac{\partial x}{\partial \theta_B}$$

So

$$\left(\frac{\partial y}{\partial \eta}\right)^2 = \left(\frac{\partial x}{\partial \theta_B}\right)^2$$

Hence

$$g_\eta = g_{\theta_B}$$

Substituting

$$g_\eta = \left[\frac{a(1 - \cos \theta_B \cosh \eta)}{(\cosh \eta - \cos \theta_B)^2}\right]^2 + \left[\frac{a \sin \theta_B \sinh \eta}{(\cosh \eta - \cos \theta_B)^2}\right]^2$$

Factoring and simplifying

$$g_\eta = a^2 \frac{1 - 2\cos \theta_B \cosh \eta + \cos^2\theta_B \cosh \eta + \sin^2\theta_B \sinh^2 \eta}{(\cosh \eta - \cos \theta_B)^4}$$

Substituting

$$\cos^2\theta_B = 1 - \sin^2\theta_B$$

$$\sinh^2\eta = \cosh^2\eta - 1$$

gives

$$g_\eta = a^2 \frac{\cos^2 \theta_B - 2\cos \theta_B \cosh \eta + \cosh^2 \eta}{(\cosh \eta - \cos \theta_B)^4}$$

70

Therefore

$$g_\eta = a^2 \frac{(\cosh \eta - \cos \theta_B)^2}{(\cosh \eta - \cos \theta_B)^4} = \frac{a^2}{(\cosh \eta - \cos \theta_B)^2}$$

So

$$g_{\theta_B} = g_\eta = \frac{a^2}{(\cosh \eta - \cos \theta_B)^2}$$

Also

$$g = g_{\theta_B} g_\eta = \frac{a^4}{(\cosh \eta - \cos \theta_B)^4}$$

And

$$g^{1/2} = (g_{\theta_B} g_\eta)^{1/2} = g_\eta = \frac{a^2}{(\cosh \eta - \cos \theta_B)^2}$$

Generally, the Laplacian is written (as in Appendix A but for two dimension)

$$\nabla^2 \varphi = g^{-1/2} \left\{ \frac{\partial}{\partial x_1} \left[\frac{g^{1/2}}{g_{11}} \frac{\partial \varphi}{\partial x_1} \right] + \frac{\partial}{\partial x_2} \left[\frac{g^{1/2}}{g_{22}} \frac{\partial \varphi}{\partial x_2} \right] \right\}$$

Substituting

$$\nabla^2 \varphi = g^{-1/2} \left\{ \frac{\partial}{\partial \eta} \left[\frac{g^{1/2}}{g_\eta} \frac{\partial \varphi}{\partial \eta} \right] + \frac{\partial}{\partial \theta_B} \left[\frac{g^{1/2}}{g_{\theta_B}} \frac{\partial \varphi}{\partial \theta_B} \right] \right\}$$

But

$$g^{1/2} = g_\eta = g_{\theta_B}$$

Hence

$$\nabla^2 \varphi = g^{-1/2} \left\{ \frac{\partial^2 \varphi}{\partial \eta^2} + \frac{\partial^2 \varphi}{\partial \theta_B^2} \right\}$$

For our problem

$$\nabla^2 \varphi = 0$$

Therefore, dividing by $g^{1/2}$, we are back to Laplace's equation (but in the coordinates η, θ_B)

$$\frac{\partial^2 \varphi}{\partial \eta^2} + \frac{\partial^2 \varphi}{\partial \theta_B^2} = 0$$

71

But we picked η and θ_B to force the potential to be a function of η only. So

$$\frac{d^2\varphi}{d\eta^2} = 0$$

is the appropriate differential equation, the solution of which is trivial

$$\varphi = A + B\eta$$

Consider two long parallel metal cylinders with radii r_1 and r_2 and potentials V_1 and V_2, respectively. They cylinders are on the opposite sides of the y-axis. Designate the two cylinders by η_1 and η_2. Then the boundary conditions are

$$\begin{Bmatrix} \eta = \eta_1 , & \varphi = V_1 \\ \eta = \eta_2 , & \varphi = V_2 \end{Bmatrix}$$

Substitution of the boundary conditions leads to

$$\varphi = \frac{1}{\eta_1 - \eta_2} \left\{ (V_2\eta_1 - V_1\eta_2) + (V_1 - V_2)\eta \right\}$$

The electric field strength is

$$\vec{E} = -\,\text{grad}\ \varphi = -\frac{\vec{a\eta}}{(g\eta)^{\frac{1}{2}}} \frac{d\varphi}{d\eta}$$

where

$$\frac{d\varphi}{d\eta} = \left(\frac{V_1 - V_2}{\eta_1 - \eta_2} \right)$$

and

$$(g\eta)^{\frac{1}{2}} = \frac{a}{\cosh \eta - \cos \theta_B}$$

So

$$\vec{E} = -\,\vec{a\eta}\, \frac{(V_1 - V_2)}{a(\eta_1 - \eta_2)} (\cosh \eta - \cos \theta_B)$$

It will be found useful to have the x and y components of the field strength as well

$$E_x = -\frac{\partial \varphi}{\partial x}$$

and

72

$$E_y = -\frac{\partial \varphi}{\partial y}$$

From calculus

$$\frac{\partial \varphi}{\partial x} = \frac{\partial \varphi}{\partial \eta}\bigg)_{\theta_B} \frac{\partial \eta}{\partial x}\bigg)_y + \frac{\partial \varphi}{\partial \theta_B}\bigg)_\eta \frac{\partial \theta_B}{\partial x}\bigg)_y$$

and

$$\frac{\partial \varphi}{\partial y} = \frac{\partial \varphi}{\partial \eta}\bigg)_{\theta_B} \frac{\partial \eta}{\partial y}\bigg)_x + \frac{\partial \varphi}{\partial \theta_B}\bigg)_\eta \frac{\partial \theta_B}{\partial y}\bigg)_x$$

But

$$\frac{\partial \varphi}{\partial \theta_B} = 0$$

Hence

$$\frac{\partial \varphi}{\partial x} = \frac{\partial \varphi}{\partial \eta} \frac{\partial \eta}{\partial x}$$

and

$$\frac{\partial \varphi}{\partial y} = \frac{\partial \varphi}{\partial \eta} \frac{\partial \eta}{\partial y}$$

Again,

$$\eta = \ell n \frac{\sqrt{(x^2+y^2-a^2)^2 + (2ay)^2}}{(x-a)^2 + y^2}$$

After simplifications,

$$\frac{\partial \eta}{\partial x} = \frac{[(x-a)^2 + y^2](x^2+y^2-a^2)2x - [(x^2+y^2-a^2)^2 + (2ay)^2]2(x-a)}{[(x^2+y^2-a^2)^2 + (2ay)^2][(x-a)^2 + y^2]}$$

$$\frac{\partial \eta}{\partial y} = 2y \frac{[(x-a)^2 + y^2](x^2+y^2+a^2) - [(x^2+y^2-a^2)^2 + (2ay)^2]}{[(x^2+y^2-a^2)^2 + (2ay)^2][(x-a)^2 + y^2]}$$

The derivatives simplify further to

$$\frac{\partial \eta}{\partial x} = 2\left\{ \frac{x^2 + y^2 - a^2}{[(x^2+y^2-a^2)^2 + (2ay)^2]} - \frac{(x-a)}{[(x-a)^2 + y^2]} \right\}$$

73

$$\frac{\partial \eta}{\partial y} = 2y\left\{\frac{x^2 + y^2 + a^2}{[(x^2+y^2-a^2)^2 + (2ay)^2]} - \frac{1}{[(x-a)^2 + y^2]}\right\}$$

So, substituting, and letting $V = V_1 - V_2$

$$E_x = -\frac{V}{(\eta_1 - \eta_2)} \cdot 2\left\{\frac{x(x^2+y^2-a^2)}{[(x^2+y^2-a^2)^2 + (2ay)^2]} - \frac{(x-a)}{[(x-a)^2 + y^2]}\right\}$$

$$E_y = -\frac{V}{(\eta_1 - \eta_2)} \cdot 2y\left\{\frac{x^2 + y^2 + a^2}{[(x^2+y^2-a^2)^2 + (2ay)^2]} - \frac{1}{[(x-a)^2 + y^2]}\right\}$$

where

$$\eta_i = \sinh^{-1}\frac{a}{r_i} ; \qquad i = 1,2$$

It is now necessary to determine the pole (a) as a function of the radii (r_1, r_2) and the distance between the centers of the cylinders (S). Call the distance from the origin to the cylinder centers d_1 and d_2. Hence (Reference 9)

$$d_1 = a \coth \eta_1 , \qquad d_2 = a \coth \eta_2$$

In general

$$d = a \coth \eta = a \frac{\cosh \eta}{\sinh \eta} = a \frac{(\sinh^2\eta + 1)^{1/2}}{\sinh \eta}$$

But

$$\sinh \eta = a/r$$

Therefore

$$d = a \cdot \frac{[(a/r)^2 + 1]^{1/2}}{a/r} = (a^2+r^2)^{1/2}$$

So the spacing S between axes of cylinders is

$$S = d_2 - d_1 = (a^2+r_2^2)^{1/2} + (a^2+r_1^2)^{1/2}$$

Solving this equation for a gives

$$a = \frac{1}{2S}\left[S^4 - 2S^2(r_1^2 + r_2^2) + (r_2^2-r_1^2)^2\right]^{1/2}$$

74

Knowing that

$$\sinh^{-1}u = \ell n \left[u + (u^2+1)^{\frac{1}{2}} \right]$$

The values for η_1, η_2 can be computed

$$\eta_i = \pm \, \ell n \left[\frac{a}{r_i} + \left(\frac{a^2}{r_i^2} + 1 \right)^{\frac{1}{2}} \right] ; \quad i = 1,2$$

The sign is determined by the side (positive or negative) of the y axis the cylinder is located. This is an arbitrary choice. Choose cylinder No. 1 to be on the negative side and cylinder No. 2 to be on the positive. Then

$$\eta_1 = - \, \ell n \left[\frac{a}{r_1} + \left(\frac{a^2}{r_1^2} + 1 \right)^{\frac{1}{2}} \right] \tag{14}$$

$$\eta_2 = \ell n \left[\frac{a}{r_2} + \left(\frac{a^2}{r_1^2} + 1 \right)^{\frac{1}{2}} \right] \tag{15}$$

Hence, given any two cylinders with radii (r_1, r_2) and center-center distance (S), the electric field components may be computed for any position. (References 1, 9, 11, 14).

75

APPENDIX C

NUMERICAL SOLUTION EQUATIONS AND COMPUTER PROGRAM

Preceding page blank

All the streamline differential equations (with or without the simultaneous velocity equations) were solved using the <u>Runge-Kutta third order approximation</u>. (Reference 17).

In general, the simultaneous equations,

$$\frac{dy}{dx} = f(x,y,t) \quad , \quad \frac{dx}{dt} = g(x,y,t)$$

at intervals $\Delta x = h$, can be solved using

$$k_1 = f(x_0, y_0, t_0)h$$

$$\ell_1 = g(x_0, y_0, t_0)h$$

$$k_2 = f(x_0 + 1/3h, y_0 + 1/3k_1, t_0 + 1/3\ell_1)h$$

$$\ell_2 = g(x_0 + 1/3h, y_0 + 1/3k_1, t_0 + 1/3\ell_1)h$$

$$k_3 = f(x_0 + 2/3h, y_0 + 2/3k_2, t_0 + 2/3\ell_2)h$$

$$\ell_3 = g(x_0 + 2/3h, y_0 + 2/3k_2, t_0 + 2/3\ell_2)h$$

and then using the formulas

$$\Delta y = \frac{1}{4}(k_1 + 3k_3)$$

$$\Delta t = \frac{1}{4}(\ell_1 + 3\ell_3)$$

to solve for the new point.

For the steady state cases (1) and (3), only the Δy equation is necessary for solution. If the various increments are computed in the indicated order, each involves only quantities which have been previously calculated.

The error for each calculation is of the order of $(\Delta x)^4$.

Considering the longest path an ion would be expected to take and allowing the maximum error for this path to be approximately .002, the interval for which the equations were solved (Δx or Δy) was <u>.08</u>.

The program was written so that if the value of the derivative was less than one, the interval was taken in the x-direction, and if the derivative was greater than one, the interval was taken in the y-direction.

Preceding page blank

79

This was done to minimize the total error. Also, if the velocity was in the positive x or y-direction the interval was positive and if the velocity was in the negative directions the interval was negative.

List of Program Symbols:

$$A = r_2$$

$$B = d_2$$

$$C = a$$

$$DN = K_0$$

$$V = V$$

$$U = U$$

$$JJ = \text{ion count}$$

$$E1 = \eta_1$$

$$E2 = \eta_2$$

$$DM = M$$

$$P = t$$

$$W = \alpha$$

$$ADYDX = \frac{dy'}{dx'}$$

$$VIX = V_{IX}$$

$$VIY = V_{IY}$$

$$DELX = \Delta x$$

$$DELY = \Delta y$$

$$DD = \frac{dy'}{dx'} \text{ or } \frac{dx'}{dy'}$$

$$YO = y_0$$

$$XO = x_0$$

$Po = t_O$

$R_1 = k_1$

$R_2 = k_2$

$R_3 = k_3$

$S_1 = l_1$

$S_2 = l_2$

$S_3 = l_3$

RAD = distance from cylinder center to ion

ANG = γ

The program included is for case (2), unsteady circulation, constant mobility.

```
- SEXECUTE      PUFFT
  SPUFFT    99,
          DIMENSION JJ(15)
          DO 888 N=1,15
 888      JJ(N)=0
          DN=1.31
          V=20.*(10.**3.)
          A=6.6656
          B=7.22
          C=2.78
          E1=-4.01
          E2=.406
          U=1780.
          IF(U)160,150,160
 160      DM=V*DN/((E2-E1)*U*A)
          WRITE(6,2)DM
 2        FORMAT(20X,F10.4)
 150      DO 100 J=1,26
          DO 300 M=1,6
          P=(.0794/6.)*FLOAT(M-1)
          W=.6666*3.1416+(3.1416/150.)*FLOAT(J-1)
          Y=.1*SIN(W)
          X=-C+.1*COS(W)
 6        ADYDX=ABS(VIY(X,Y,U,P)/VIX(X,Y,U,P))
          IF(ADYDX-1.)20,20,30
 20       IF(VIX(X,Y,U,P))40,40,50
 40       DELX=-.08
          GO TO 130
 50       DELX=.08
 130      DD=VIY(X,Y,U,P)/VIX(X,Y,U,P)
          YO=Y
          XO=X
          PO=P
          R1=DELX*DD
          S1=ABS(DELX/VIX(X,Y,U,P))
          X=XO+DELX/3.
          Y=YO+R1/3.
          P=PO+S1/3.
          DD=VIY(X,Y,U,P)/VIX(X,Y,U,P)
          R2=DELX*DD
          S2=ABS(DELX/VIX(X,Y,U,P))
          X=XO+.6666*DELX
          Y=YO+.6666*R2
          P=PO+.6666*S2
          DD=VIY(X,Y,U,P)/VIX(X,Y,U,P)
          R3=DELX*DD
          S3=ABS(DELX/VIX(X,Y,U,P))
          X=XO+DELX
```

82

```fortran
        Y=YO+.25*(R1+3.*R3)
        P=PO+.25*(S1+3.*S3)
        GO TO 80
   30   IF(VIY(X,Y,U,P))60,60,70
   60   DELY=-.08
        GO TO 140
   70   DELY=.08
  140   DD=VIY(X,Y,U,P)/VIX(X,Y,U,P)
        YO=Y
        XO=X
        PO=P
        R1=DELY/DD
        S1=ABS(DELY/VIY(X,Y,U,P))
        Y=YO+DELY/3.
        X=XO+R1/3.
        P=PO+S1/3.
        DD=VIY(X,Y,U,P)/VIX(X,Y,U,P)
        R2=DELY/DD
        S2=ABS(DELY/VIY(X,Y,U,P))
        Y=YO+.6666*DELY
        X=XO+.6666*R2
        P=PO+.6666*S2
        DD=VIY(X,Y,U,P)/VIX(X,Y,U,P)
        R3=DELY/DD
        S3=ABS(DELY/VIY(X,Y,U,P))
        Y=YO+DELY
        X=XO+.25*(R1+3.*R3)
        P=PO+.25*(S1+3.*S3)
   80   RAD=SQRT((X-B)*(X-B)+Y*Y)
        IF(X-4.)777,300,300
  777   IF(RAD-A)666,666,6
  666   ANG=ATAN(Y/(B-X))
        IF(ANG-.873)300,555,555
  555   IF(ANG-.996)444,444,300
  444   JJ(M)=JJ(M)+1
  300   CONTINUE
  100   CONTINUE
        WRITE(6,77) (JJ(KJ),KJ=1,15)
   77   FORMAT(10X,15I4)
    7   STOP
        END
        FUNCTION VIX(X,Y,U,P)
        A=6.6666
        B=7.22
        C=2.78
        E1=-4.01
        E2=.406
        DN=1.31
        V=20.*(10.**3.)
        E=X*X+Y*Y-C*C
```

83

```
      F=E*E+4.*C*C*Y*Y
      G=(X-C)*(X-C)+Y*Y
      DEDX=2.*((X*E/F)-((X-C)/G))
      EX=V*DEDX/(E2-E1)
      TP=79.1*P
      VFX=U*(1.+(A*A)*(Y*Y-(X-B)*(X-B))/(((X-B)*(X-B)+Y*Y)
     1((X-B)*(X-B)+Y*Y)))
     1+1.5*U*A*Y*SIN(TP)/(6.2832*((X-B)*(X-B)+Y*Y))
      D=DN
      VIX=VFX+D*EX
      RETURN
      END
      FUNCTION VIY(X,Y,U,P)
      A=6.6666
      B=7.22
      C=2.78
      E1=-4.01
      E2=.406
      DN=1.31
      V=20.*(10.**3.)
      E=X*X+Y*Y-C*C
      F=E*E+4.*C*C*Y*Y
      G=(X-C)*(X-C)+Y*Y
      H=X*X+Y*Y+C*C
      DEDY=2.*Y*((H/F)-(1.7G))
      EY=V*DEDY/(E2-E1)
      TP=79.1*P
      VFY=-2.*A*A*U*((Y*(X-B))/(((X-B)*(X-B)+Y*Y)*((X-B)
     1*(X-B)+Y*Y)))
     1-1.5*U*A*SIN(TP)*(X-B)/(6.2832*((X-B)*(X-B)+Y*Y))
      D=DN
      VIY=VFY+D*EY
      RETURN
      END
$DATA
```

APPENDIX D

ANALYSIS OF ION TRAJECTORIES FOR

TWO SIMPLE POTENTIAL FLOW CASES

The general method developed in the body of this work may be used for any corona wire geometry or flow case (the fluid flow may be viscous or inviscid). To demonstrate the nature of the technique two simple cases will be studied.

The first case has an infinite row of corona wires opposite to an infinite conducting plate. The fluid flow is directed perpendicular to the plate.
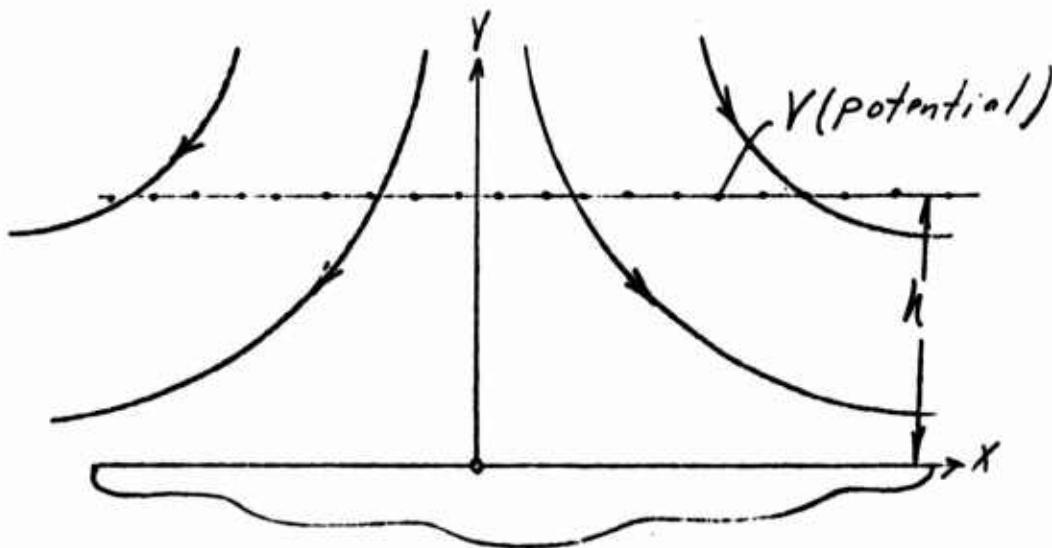

Figure 28. Infinite Row of Corona Wires
Opposite Infinite Plate

The electric field is taken to be constant between the wires and the plate.

$$E_y = -\frac{V}{h}, \quad E_x = 0$$

The complex potential for this flow is (Reference 15)

$$W_F = \varphi_F + i\psi_F = Az^2$$

Substituting $Z = x + iy$ and separating the equation into real and imaginary parts gives

$$\varphi_F = A(x^2 - y^2), \quad \psi_F = 2Axy$$

The fluid velocities are then

$$V_{Fx} = -\frac{\partial \varphi_F}{\partial x} = -2Ax$$

and

$$V_{Fy} = -\frac{\partial \varphi F}{\partial y} = 2Ay$$

The ion transport velocity components are

$$V_{Ix} = V_{Fx} + K\,E_x$$

$$V_{Iy} = V_{Fy} + K\,E_y$$

and the streamline differential equation is

$$\frac{dy}{dx} = \frac{V_{Fy} + K\,E_y}{V_{Fx} + K\,E_x}$$

Hence, substituting,

$$\frac{dy}{dx} = \frac{2Ay - \frac{KV}{h}}{-2Ax}$$

Let $y' = \frac{y}{h}$, $x' = \frac{x}{h}$, therefore

$$\frac{dy'}{dx} = -\frac{2Ahy' - \frac{KV}{h}}{2Ahx'}$$

Dividing the numerator and denominator by 2Ah' gives

$$\frac{dy'}{dx'} = -\frac{y' - \frac{KV}{2Ah^2}}{x'}$$

Rearranging,

$$\frac{dy'}{y' - \frac{KV}{2Ah^2}} = -\frac{dx'}{x'}$$

Integration yields

$$\ell n\left(y' - \frac{KV}{2Ah^2}\right) + \ell n\ X' = C'$$

Or

$$\left(y' - \frac{KV}{2Ah^2}\right)X' = C$$

88

One dimensionless parameter controls this case.

$$\frac{KV}{2Ah^2}$$

Note that A is negative for the flow being studied. If $\left|\frac{KV}{2Ah^2}\right|$ is negligible compared to unity (the maximum value of y' is unity), the trajectory equation yields a family of hyperbolas. If $\left|\frac{KV}{2Ah^2}\right|$ is much greater than unity, the equation gives x' equal to a constant (the ions are travelling perpendicular in straight lines to the plate).

The second case has two concentric conducting cylinders enclosing a potential vortex.
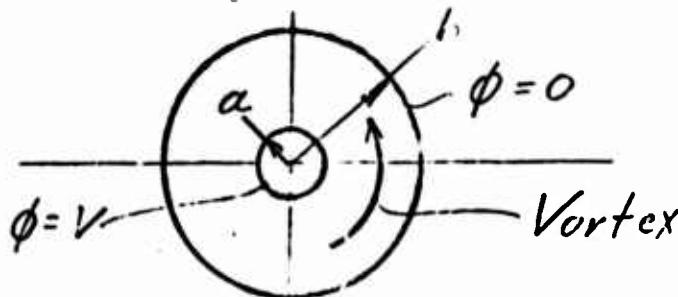
Figure 29. Two Cylinders Enclosing Vortex

The electric field for this case is radial and is given by (Reference 14)

$$\vec{E} = E_r = - \vec{a}_r \frac{V}{\ell n \frac{b}{a}} \frac{1}{r} , E_\theta = 0$$

The complex vortex potential is (Reference 15)

$$W_F = iu\ell n(Z - Zo)$$

Zo = 0, hence

$$W_F = iu\ell n(Z) = iu\ell n(re^{i\theta})$$

So

$$\varphi_F + i\varphi_F = iu\ell n(r) - u\theta$$

Therefore

$$\varphi_F = - u\theta$$

89

The fluid velocity components in polar coordinates are

$$V_{F\theta} = -\frac{1}{r}\frac{\partial \varphi F}{\partial \theta}, \quad V_{Fr} = -\frac{\partial \varphi F}{\partial r}$$

Hence,

$$V_{F\theta} = \frac{1}{r}u, \quad V_{Fr} = 0$$

Consequently

$$V_{I\theta} = r\frac{d\theta}{dt} = V_{F\theta} = -\frac{1}{r}u$$

and

$$V_{Ir} = \frac{dr}{dt} = KE_r = \frac{KV}{\ell n\frac{b}{a}}\frac{1}{r}$$

$$\frac{dr}{d\theta} = \frac{\frac{dr}{dt}}{\frac{d\theta}{dt}} = \frac{\frac{KV}{\ell n\frac{b}{a}}\frac{1}{r}}{\frac{u}{r^2}} = \frac{KV}{\ell n\frac{b}{a}u}r$$

Let $r' = \frac{r}{b}$, θ is already dimensionless

so

$$b\frac{dr'}{d\theta} = \frac{KV}{\ell n\frac{b}{a}u}br'$$

and

$$\frac{dr'}{r'} = \frac{KV}{\ell n\frac{b}{a}u}d\theta$$

Integrating,

$$\ell n r' = \frac{KV}{\ell n\frac{b}{a}u}\theta + c'$$

which may be written

$$r' = c\ e^{\frac{KV}{\ell n\frac{b}{a}u}\theta}$$

90

which is obviously a spiral. This case also has one dimensionless parameter

$$\frac{KV}{\ln \frac{b}{a}\, u}$$

Substituting initial conditions of $r' = \frac{a}{b}$ and $\theta = 0$ gives

$$r' = \frac{a}{b}\, e^{\frac{KV}{\ln \frac{b}{a}\, u}\, \theta}$$

as the trajectory equation.

APPENDIX E

BICYLINDRICAL COORDINATES

93
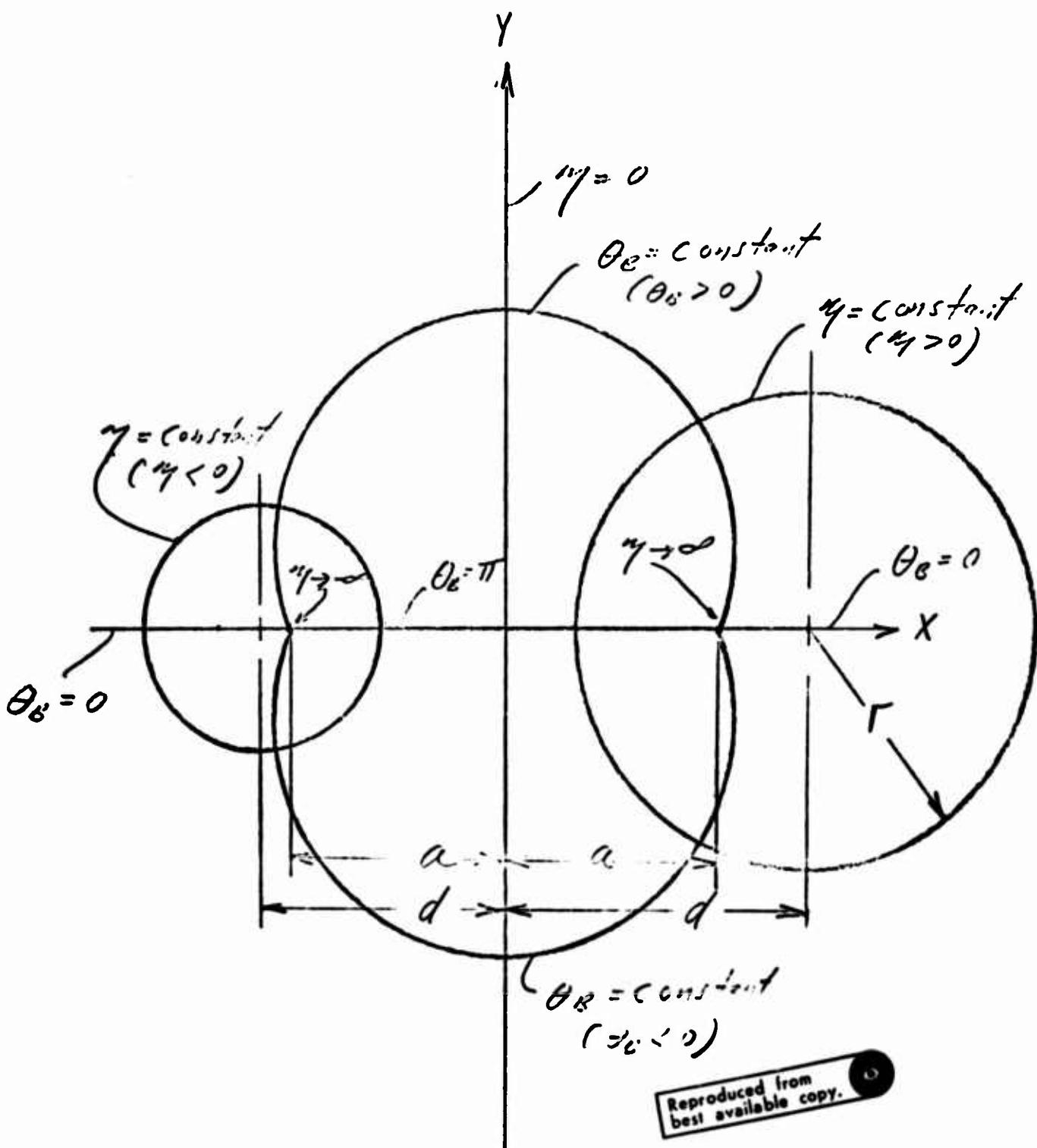
Figure 30. Bicylindrical Coordinates. The lines η = constant are
circles with axes on the x-axis. The lines θ_B = constant
are portions of circles with axes on the y axis.
(Reference 9).

94

APPENDIX F

A FLUID-ELECTRICAL STREAM FUNCTION

All the trajectory analyses undertaken in this work have been primarily the solution of the differential equation

$$\frac{dy}{dx} = \frac{V_{Fy} + K E_y}{V_{Fx} + K E_x}$$

Another method of determining the ion trajectories for steady flow which will lead to closed solutions is simply adding the stream function of the fluid flow (ψ_F) to the product of the mobility times the stream function of the electrical field (ψ_E). This sum yields a combined fluid-electrical stream function (ψ_{FE}) which may then be solved for the trajectories.

$$\psi_{FE} = \psi_F + K\psi_E$$

In general, I would state that this method is valid for steady state, constant mobility ion flow problems.

APPENDIX G

ABSTRACT OF EXPERIMENTAL TESTS OF FLUID FLOW DIAGNOSTICS

USING ELECTROSTATIC CHARGES

Studies were initiated into the possible use of charged particles in a gas stream as a means of studying the nature of gas flow. Two basic approaches were followed. In one case, ions were generated electrostatically by means of a corona discharge from a suitable point or line source. In the second case, the charges were obtained either from the natural dust or water particles in the air, or dust particles were deliberately added to the air stream. The charges were collected at selected positions downstream on the particular aerodynamic shape being studied.

Experimental Study With Ions

Three configurations have been studied. They include a six-inch-diameter cylinder mounted transverse to the air stream, a three-foot-long sharp-edged flat plate, and an NACA 0012 airfoil of 0.216 m chord length, all of which were mounted in the U. S. Army AMRDL 7 x 10 tunnel at Ames Research Center and tested at various tunnel speeds. Most of the runs were made using a 0.0038 cm diameter corona wire placed a few centimeters upstream of the surface. Electric field shaping electrodes adjacent to the wire were grounded. Strips of alumimum 1.25 cm wide, foil spaced at 0.32 cm were mounted on each surface. An end view of one configuration is shown in Figure 31. The filter is used to eliminate background 60 Hz noise.
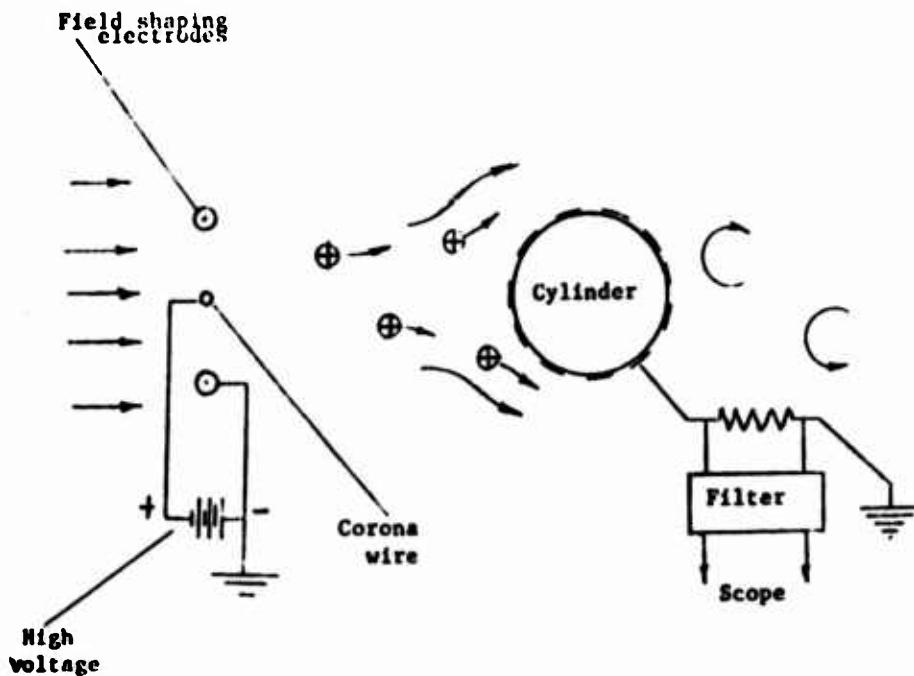

Figure 31. Ion-Flow Measurement Scheme

The corona currents ranged from 2 μA to 30 μA and the applied potential used to get the corona ranged from 6 to 16 kV which depended mainly on the configuration of the electrodes. Essentially the same results were achieved regardless of the currents used.

Figure 32 shows a typical oscilloscope trace using the cylinder at a tunnel q of one. The upper traces are taken from the resistor connected to the most forward position on the cylinder and the lower grace is from the most aft position. The regularity of the upper traces indicates that the ion currents tend to follow the basic oscillating flow about a cylinder in cross flow. Such flow oscillations are the result of the periodic shedding of vortices from a cylinder. At the rear of the cylinder the flow has largely separated and close to the cylinder is essentially a "dead-water" region. Examination of the lower trace reveals that the current oscillation is reduced greatly or eliminated. The frequency of the oscillation is 16 Hz which is of the correct order for the Strouhal frequency for this cylinder. Thus, the ion technique in this case seems to respond properly to the characteristics of the flow field.
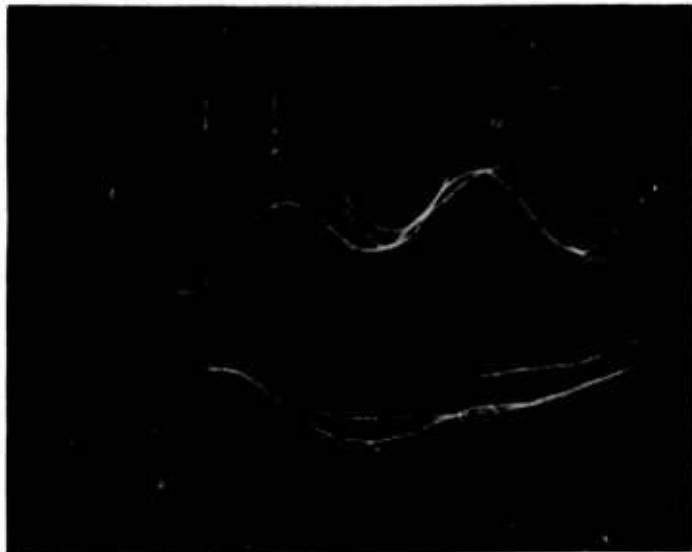

Figure 32. Circular Cylinder Trace

Next, a flat plate was placed directly aft of the cylinder at the centerline and extended 0.46 m rearward. Such surfaces act to eliminate or reduce the periodic shedding. Figure 33 shows the results using the ion technique. The upper trace is from the front of the cylinder and it can be seen that the ion technique indeed does show greatly reduced oscillation.
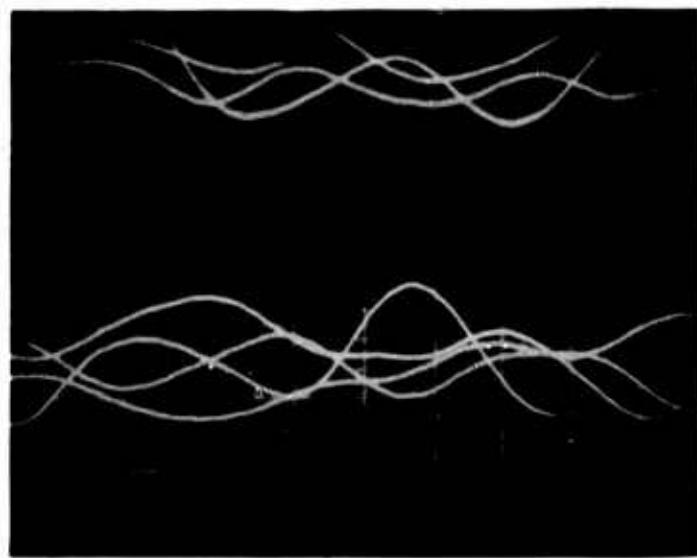

Figure 33. Circular Cylinder With Aft Plate

The three-foot-long sharp-edged flat plate was mounted in the tunnel parallel to the windstream. The electrodes were located on the upper surface. The top trace of Figure 34 illustrates an oscillation in flow 0.10 m aft of the leading edge. These oscillations may indicate the presence of a separation bubble near the leading edge. The next trace from a position 3.8 cm aft of the first trace, although it shows excursions, does not show oscillations. The lowest trace further back on the plate shows a relatively smooth appearance. The ion technique seems to give a proper indication of the flow for this case.
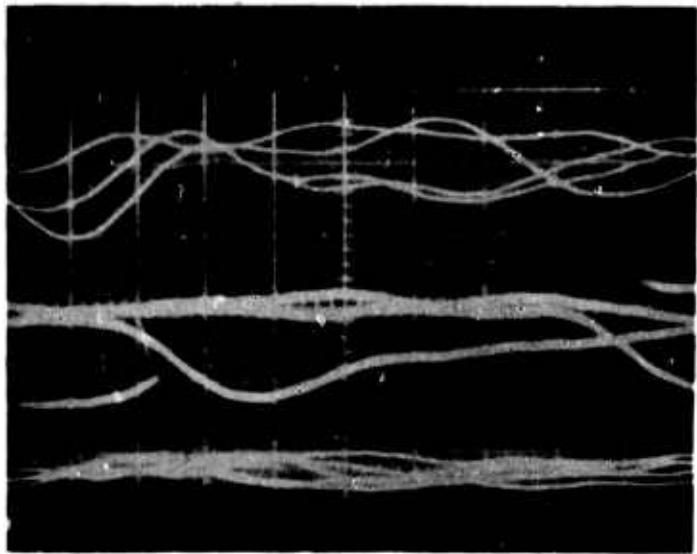
Figure 34.   Sharp-Edged Flat Plate

Tests next were run on the airfoil using the corona wire and field-shaping electrodes. Current collecting strips were located over the entire airfoil. At a tunnel q of one (8.2 m/sec) and an angle of attack of 0°, all the traces from positions around the airfoil were smooth and regular except at one location. The upper trace of Figure 35 is 10.8 cm from the nose of the airfoil. The next two traces are 1.6 cm and 3.2 cm further back on the 0.216 m chord airfoil. It can readily be seen that a significant oscillation exists within a limited region on the airfoil, indicating the presence of a separation zone. Thus, the ion technique appears to be able to discriminate local phenomenon. All the foregoing ion-flow tests were taken with a filter setting which filtered out frequencies about 30 Hz. This is the reason why no high frequency oscillations appear in the data.

Another test using the airfoil set at an angle of attack of 17° and a tunnel q of 10 (V = 26 m/sec) was : in with the filter set to pass frequencies in the 150-2000 Hz range. Figure 36 illustrates violent oscillations of the ion currents at two positions near the midchord region of the upper surface. This action is expected since the airfoil is in full stall. The lower surface traces show relatively random behavior with peak amplitudes of approximately 1-5% of the upper surface trace amplitudes.

104
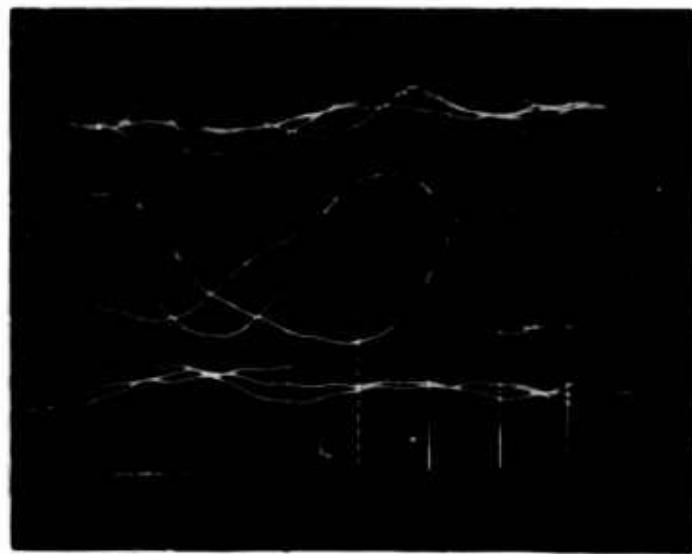
Figure 35.   Airfoil at 0° Angle
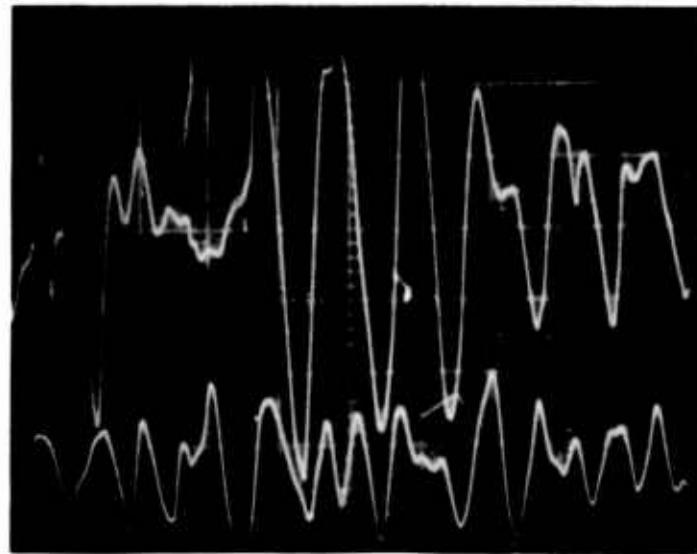
Figure 36.   Airfoil at 17° Angle

105

Charged Particles Tests

The next phase consisted of using the charged particles carried in the wind tunnel stream as the source of charge. The configuration used was the cylinder with the rear splitter plate. The electrode at the rear edge of the plate was monitored. Large oscillations can be noted from the trace in Figure 37. The flow in this region contains large scale turbulence and such large scale oscillations are expected. If corona currents are used with this test configuration, similar oscillations are seen but their magnitude is several times greater.

Figure 37. Charged Particle Traces